Acknowledgements

"Success is not final, failure is not fatal; it is the courage to continue that counts"
- *Winston Churchill*

Abstract

Seabird populations are sensitive to changes in their environment and can therefore be studied as indicators of ecosystem health. Meanwhile, drone technologies have become popular in ecological studies, and there is potential for using drones to track seabirds to assess ecosystem health, yet first they must be tested for proof-of-concept. In this pilot study, three instrument carrying platforms (bio-drone, aerial drone, and underwater drone) were deployed near a European shag *Phalacrocorax aristotelis* colony at Runde (62.4006 N, 5.6242 E), Norway, in June 2017. Some selected European shags were used as "bio-drones", i.e. carriers of small loggers for geographical information and time-depth recorders to indicate the activity of the birds and their diving locations. The areas with bio-drone activity were the basis for further mapping using other drones, i.e. an Unmanned Aerial Vehicle (UAV, aerial drone), and for underwater information in the diving areas a Remotely Operated Vehicle (ROV), to assess their potential for mapping of European shag foraging habitats. An additional examination of the effect of inherent optical properties (IOP) on the UAVs ability to identify an object of interest in the water column was later completed in the Trondheimsfjord, using Secchi disks of different colors mounted on the ROV. The bio-drones, with additional diet samples, provided relevant information on shag foraging behavior, and were an important first step in the three part approach using three instrument carrying platforms (bio-drones, UAV, and ROV) for mapping and monitoring of the European shag population. The ROV was found to be an effective supplement to the information from the bio-drones, as it provided insight into bottom substrate types and depths, as well as *in situ* observations of potential prey species diversity in the survey area. Using the ROV and UAV together proved advantageous compared to using the ROV by itself, as the UAV was able to guide the ROV to avoid collisions with obstacles and maintain its trajectory. The UAV's imaging capability were found to be variable due to the effect of light, IOP, and distance to the different objects of interest on image quality, as well as its vulnerability to weather conditions. Despite the challenges, the UAV, both alone and in combination with ROV and bio-drone technologies, holds potential for improved mapping and monitoring of seabirds. To ascertain the extent to which UAVs can be used to map the marine environment, further studies of the technology should be completed with a more weather resistant UAV model and with a multi- or hyperspectral imaging sensor to reduce the impact of study area conditions on image quality.

Sammendrag

Sjøfuglpopulasjoner er sensitive til forandringer i sitt miljø. De kan derfor studeres som indikatorer for endringer i økosystemer. I mellomtiden har droneteknologier økt i viktighet som verktøy i økologistudier og de har potensiale som viktige verktøy i økosystemstudier, men først må de testes for «proof-of-concept». I denne pilotstudien ble tre instrumentbærende plattformer (bio-drone, luftdrone, og undervannsdrone) tatt i bruk nær toppskarv *Phalacrocorax aristotelis* kolonien på Runde (62.4006 N, 5.6242 E), Norge, i juni 2017. Noen toppskarver ble brukt som «bio-droner», altså bærere av små loggere av geografisk informasjon og tid-dybde målere for å indikere aktiviteten til fuglene og deres dykkeområder. Områdene med bio-droneaktivitiet dannet grunnlaget for videre kartlegging med andre droner, i.e. en luftdrone (UAV) og en fjernstyrt undervannsfarkost (ROV) for å vurdere deres potensiale til å kartlegge toppskarvens jaktområder. En tilleggsstudie av effekten av de iboende optiske egenskapene (IOP) til vann på UAV-ens evne til å gjenkjenne objekter av interesse i vannkollonnen ble senere gjennomført i Trondheimsfjorden med Secchi-skiver i forskjellige farger montert på ROV-en. Bio-dronene, med ytterligere diettprøver, ga verdifull informasjon om jaktoppførsel hos toppskarvene, og de var et viktig første steg i den tredelte tilnærmingen til kartlegging med av toppskarv populasjonen ved bruk av tre instrumentbærende platformer (bio-droner, UAV og ROV). ROV-en var et effektivt supplement til informasjonen fra bio-dronene, da den ga innblikk i substrattyper og dybde, samt *in situ* observasjoner av artsdiversitet av potensielle byttedyr i studieområdet. Bruk av ROV og UAV sammen var fordelaktig sammenlignet med kun ROV, da UAV-en kunne sørge for at ROV-en unngikk kollisjoner med hinder og så den ikke kjørte seg fast. Bildekvalitet fra UAV var avhengig av lysforhold, IOP og avstand til objektet, i tillegg til dronemodellens sårbarhet til vær. På tross av utfordringene har UAV-en potensial til å være verdifull i kartleggingsstudier av sjøfugl, både alene og i samvirke med bio-droner og ROV. For å fastsette verdien av UAV-er i kartlegging av et marint miljø, trengs videre forskning på bruk av teknologien. Disse bør gjennomføres en mer værbestandig UAV-modell, og med en multi- eller hyperspektral bildesensor for å redusere innflytelsen av miljøet i studieområdet sin effekt på bildekvalitet.

Table of Contents

List of figures

List of tables

Abbreviations

AOP	Apparent Optical Properties
ASPRS	American Society for Photogrammetry and Remote Sensing
AUV	Autonomous underwater vehicle
cDOM	Colored Dissolved Organic Matter
CEN	European Committee for Standardization
Chl-a	Chlorophyll-a
CMOS	Complementary metal–oxide–semiconductor
FoV	Field of View
GIMP	GNU Image Manipulation Program
GPS	Geographic Positioning System
IOP	Inherent Optical Properties
IOCCG	Internation Ocean Color Coordinating Group
IUCN	International Union for Conservation of Nature
NINA	Norwegian Institute for Nature Research
NGU	Geological Survey of Norway
NTNU	Norwegian University of Science and Technology
OOI	Object Of Interest
PAR	Photosynthetically Active Radiation
PF	Polarizing Filter
RGB	Red, Green, Blue
ROV	Remotely Operated Vehicle
SESAR	Single European Sky ATM Research
TBS	Trondheim Biological Station
TDR	Time Depth Recorder
TSM	Total Suspended Matter
UAV	Unmanned aerial vehicle
WoRMS	World Register of Marine Species

Terms

E_d	Downwelling irradiance
E_u	Upwelling irradiance

1. Introduction

Among the taxa suffering from anthropogenic stressors, seabirds are one of those facing the most rapid population decline (Lewison et al. 2012; Ceballos et al. 2015). Between 1950-2010, 69.7% of all globally monitored seabird populations suffered from decrease (Paleczny et al. 2015), and other studies estimate that half of all seabird species are experiencing decline (Croxall et al. 2012; IUCN 2019). The decline of seabird populations is believed to be caused by multiple factors, such as loss of habitat, rising sea temperatures, invasive species, bioaccumulation of toxins, plastic waste, and competition with fisheries (Grémillet & Boulinier 2009; Croxall et al. 2012; Lewison et al. 2012; Paleczny et al. 2015). The potential for negative interactions between humans and seabirds is especially severe in coastal areas, where humans and seabirds contend for habitat and resources (Crain, Kroeker & Halpern 2008; Warwick-Evans et al. 2016). As they are often at the top of the food web, changes in lower trophic levels or in the physicochemical environment caused by anthropogenic activities are likely to manifest themselves in seabird populations (Parsons et al. 2008).

Because of their sensitivity to changes in their environment, seabirds possess several attributes that make them potentially useful environmental indicators (Frederiksen, Mavor & Wanless 2007; Mallory et al. 2010; Lorentsen, Anker-Nilssen & Erikstad 2018). Changes in ecological factors like prey availability, habitat, and weather patterns can manifest themselves in seabird populations as changes in reproductive efforts, breeding success, or survival (Mallory et al. 2010; Bustnes et al. 2013; Lorentsen et al. 2015). Since seabirds depend on the marine environment for food and the terrestrial habitats for reproduction during the breeding season, they can be important indicators of the health status of marine ecosystems and aid in identification of important marine areas for management efforts (Frederiksen, Mavor & Wanless 2007; Parsons et al. 2008; Christensen-Dalsgaard et al. 2017). These important areas may be needed to protect estuarine and coastal systems, fisheries resources, critical habitats for endangered species, or other ecosystem services (Hyrenbach, Forney & Dayton 2000). For instance, seabird abundance trends are used by the Sustainable Development Strategies of Scotland to monitor and map and preserve important areas of biodiversity in the UK (Parsons et al. 2008). Seabird monitoring and tracking studies are becoming more widely used as the usage of indicator species becomes more popular, and the methodology for data collection is a central part of the monitoring process as it provides the data for decision and policy makers. There is therefore a need to find tracking methods and technologies appropriate for seabird

monitoring, taking into account which variables are desired, the economic and time constraints of the study, and reducing seabird disturbance (Frederiksen, Mavor & Wanless 2007; Warwick-Evans et al. 2016).

1.1. Tracking technologies in seabird studies

Existing methods for studies of seabird ecology have greatly improved our understanding of the effect and interactions between seabirds and key environmental variables (Wakefield, Phillips & Matthiopoulos 2009; Warwick-Evans et al. 2016). One way of studying seabirds is using novel tracking technologies that provide very fine-scale location and behavioral information for a sample of individuals from a known colony (Warwick-Evans et al. 2016). These tracking technologies, also known as bio-logging, track individuals using attached sensors with the aim of understanding the animal's life under uncontrolled conditions (Naito 2004). The sensors can measure the organism's state (e.g. behavior, caloric expenditure) as well as their external environment (e.g. location, temperature, salinity, depth), providing valuable information both about the individual under study, but also the condition of their habitat (Wilmers et al. 2015). The seabirds carrying bio-loggers provide information in a similar way drones (unmanned vehicles) do, though as of yet, there are no existing sources defining organisms equipped with bio-loggers as "biological drones" or "bio-drones". Considering birds were deployed with sensors in the first World War (Fig. 1.1) to map enemy positions as a modern drone would, then birds (or other species) carrying modern data-loggers are in a way acting as biological drones.

Figure 1.1: Pigeons equipped with surveillance cameras as bio-drones in the first World War. The pigeons were used by the Bavarian army as one of the first known methods of remote sensing, acting as spies mapping enemy territory. These drones acted as providers of information, similar to birds equipped with bio-loggers acting as bio-drones (Johnsen et al. 2009).

Recently, there has been an increase in the interest for remote sensing studies using unmanned aerial vehicles (UAVs; Rodríguez et al. 2012; Borelle & Fletcher 2017). Remote sensing can be defined in broad terms as the acquisition of physical data of an object without touch or contact with the object itself, and includes all methods of obtaining pictures or other forms of electromagnetic records from a distance (Campbell & Wynne 2011). Small UAVs (<3m wingspan) have potential as safe, inexpensive, and user-friendly tools for several wildlife survey applications (Jones, Pearlstine & Percival 2006). Studies where UAVs have been used in seabird research found that the drones are highly suitable for collecting extremely fine spatial and temporal resolution data of ecological variables such as population size, species distribution, or foraging behavior (Rodríguez et al. 2012; Hodgson, Kelly & Peel 2013; Hodgson et al. 2017). UAVs have been used to document populations of gulls, terns, and penguins at known breeding sites, as well as making rapid population estimates of albatross populations at remote locations (Hodgson, Kelly & Peel 2013; Chabot & Bird 2015). While investigator presence at seabird colonies is known to have negative impacts, appropriate UAV conduct can mitigate the issues (Chabot & Bird 2015; Borelle and Fletcher 2017; Weimerskirch, Prudor & Schull 2018). However it is important to consider that there are several variables important to seabird status that cannot be detected with remote sensing such as weight, number of eggs, and diet composition.

Underwater drones, defined as any vehicle able to operate underwater without a human occupant, are also becoming more common in ecological studies and for environmental mapping and monitoring (Neves et al. 2015; Ermayanti et al. 2015; Nilssen et al. 2015). They outline the subsea environment, equipped with sensors to provide insight into abiotic factors such as salinity, water density, and temperature, but also biotic factors like animal behavior or fish biodiversity (Söffker, Sloman & Hall-Spencer 2011). Underwater drones can be autonomous underwater vehicles (AUVs) or remotely operated vehicles (ROVs) like the one used in this study (Azis et al. 2012; Nilssen et al. 2015). An ROV is a tethered, mobile, non-invasive subsea instrument carrying platform with the advantage of having high maneuverability. They are also useful in ecological studies as they can bring measuring instruments to greater depths than scuba-divers are able to, thus providing more data for subsea studies (Ludvigsen 2010; Ludvigsen et al. 2014).

1.2. Light and remote sensing

To best utilize information from aerial drones, the following sections will provide basic information regarding light conditions in air and water, which are important for the interpretations of images derived from aerial and underwater drone technologies.

Light environment is central in remote sensing and photography as it provides all the information captured by a camera (if under- and overexposure are omitted) (Johnsen et al. 2009). Light is electromagnetic radiation in the part of the solar spectrum visible to the human eye, also known as Photosynthetically Active Radiation (PAR). PAR (400-700nm) describes photons with high enough energy to drive photosynthesis (Sakshaug, Johnsen & Volent 2009). What wavelength of light a camera is able to gather information from is determined by the camera sensor, which can be hyperspectral, multispectral, or Red, Green, Blue (RGB). RGB sensors capture light within the visible range or PAR, while multi- and hyperspectral sensors can register light information outside the visible range (Johnsen et al. 2013).

1.3. Optical properties of water

The optical properties of water become an important consideration for image quality when using remote sensing of objects of interest (OOI) in the sea. The turbidity and color of seawater are highly variable depending on its biological, chemical, and geochemical content (Mobley 2010).

The optical properties of water can pertain to two classes: the inherent optical properties (IOP), and the apparent optical properties (AOP). The IOPs depend only on the medium, and include the absorption and scattering by the water molecule itself as well as three optically active constituents; chlorophyll-a, total suspended matter, and colored dissolved organic matter. (Johnsen et al. 2013; Zielinski 2013; Valle et al. 2014). Chlorophyll-a (Chl-a) is present in all photosynthesizing organisms, and can therefore be used as a proxy to indicate the biomass of photosynthesizing phytoplankton. Depending on the concentrations, Chl-a can make ocean water appear green (Falkowski & Raven 2007). Total suspended matter (TSM) can be made up of both organic and inorganic particles that are insoluble in water. TSM can turn water red or yellow, depending on the type of compound. Finally, colored dissolved organic matter (cDOM) is primarily made up of organic molecules from decaying detritus or humic acids, causing waters to turn yellow to brown (Johnsen et al. 2013). While IOP depend on the medium, AOP depend both on IOP as well as the structure of the light field (Johnsen et al. 2009).

Based on their IOP concentrations water masses are distinguished into Case I or Case II waters. Case I waters typically include oligotrophic waters, open oceans and seas, while case II encompasses more complicated coastal waters (IOCCG 2000). Case II waters are much more complex in terms of their optical properties than case I waters, making interpretation of signals and images of case II waters more difficult (Fig. 1.2; IOCCG 2000; Johnsen et al. 2009).
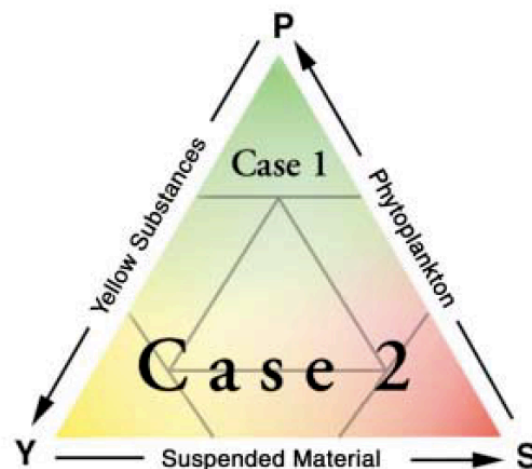
Figure 1.2: Diagrammatic representation of optically different water masses, Case I and Case II. As the figure illustrates, Case I waters tend to appear green or blue based on the phytoplankton (P) concentration, while Case II waters, also known as "green coastal waters", can range from green to yellow to brown depending on concentrations of cDOM (Y) or TSM (S) (IOCCG 2000).

1.4. Influences on image quality by water

Image quality, here referring to the level of accuracy with which an imaging system captures and displays signals that form an image, can be altered in various ways. Due to the interplay between the components affecting the optical complexity of water, problems with remote sensing both under and above the sea surface include blurring of image features, limited range of object of interest (OOI) detection, distortion and poor spatial resolution of the images, as well as particulate matter (marine snow) obscuring the OOI (Garcia, Nicosevici & Cufi 2002; Volent, Johnsen & Sigernes 2007). These factors cause scattering of light, leading to low light intensities when observing the OOI thereby lessening the image quality (Garcia, Nicosevici & Cufi 2002; Schettini & Corchs 2009). For flat surfaces such as the ocean, it is common to distinguish between downwelling (E_d) and upwelling (E_u) irradiance. Downwelling light travels down the water column, where it may be absorbed, scattered, or reflected by IOP or OOI (Fig. 1.3). As it travels through air and water, the light may weaken, so that the upwelling light moving up the water column may be dulled, influencing the remote sensor's ability to perceive the OOI or ocean color. Moreover, the IOP in the water will absorb different colors, so that the upwelling light will not only have a different intensity than the downwelling, it will also contain different color ratios (Sakshaug, Johnsen & Volent 2009).
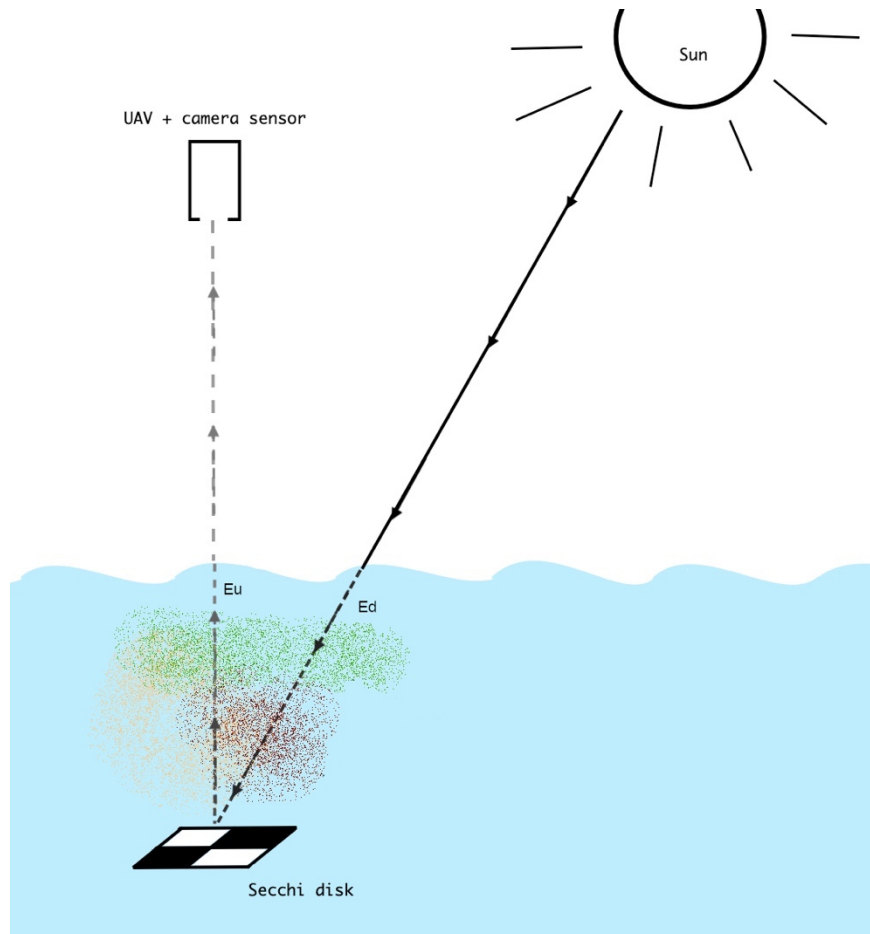
Figure 1.3: Attenuation of light intensity and color change as light passes through air and water. As light travels from source (sun) to sensor it is refracted by the ocean surface, absorbed, and/or scattered by IOP in the water (represented by red, green, and yellow colors), and the OOI in the water column. This decreases the amount of downwelling light (E_d), reaching the object, and decreases the upwelling light (E_u) reaching the sensor, making the object (e.g. Secchi disk) appear darker and harder to distinguish in images. The IOP absorb different colors, so that the upwelling light will not only have a different intensity than the downwelling, it will also contain different color ratios. Own figure.

When looking through water from above, light from the sun is reflected by the water's surface, and even miniscule waves generate irregular concentrations of irradiance (bright points) in small areas causing overexposed points in the image. These "solar glints" provide no information, but are hard to omit from the data collection (Garcia, Nicosevici & Cufi 2002; Hodgson, Kelly & Peel 2013). Overexposure may also occur and obscure information by causing glare, which is the reflection of diffuse light from skylight and clouds (Hodgson, Kelly & Peel 2013). Whereas solar glints appear more like glitter, glare causes large areas of the sea surface to become highly reflective, so that the upwelling light from beneath the surface which carries information is obscured by the more intense diffuse light reflecting off the ocean surface. Both effects can be mitigated by changing the camera's

angle in relation to the sun (or other light source), which in turn will alter the shape and orientation of the image and angle in relation to the sea surface (Hodgson, Kelly & Peel 2013).

Another factor affecting ocean color and image quality is light reflected off the substrate (Fig. 1.4). This effect, named the "bottom effect" occurs when the water is sufficiently shallow and clear so that enough light can pass through the water column then reflect off the bottom and back to the sensor. The type of substrate (sandy, rocky, coverage by benthic organisms) will affect the color of the water, providing information about the ocean floor without having to submerge a sensor, making the bottom effect useful in remote sensing in shallow regions (Volent, Johnsen & Sigernes 2007).
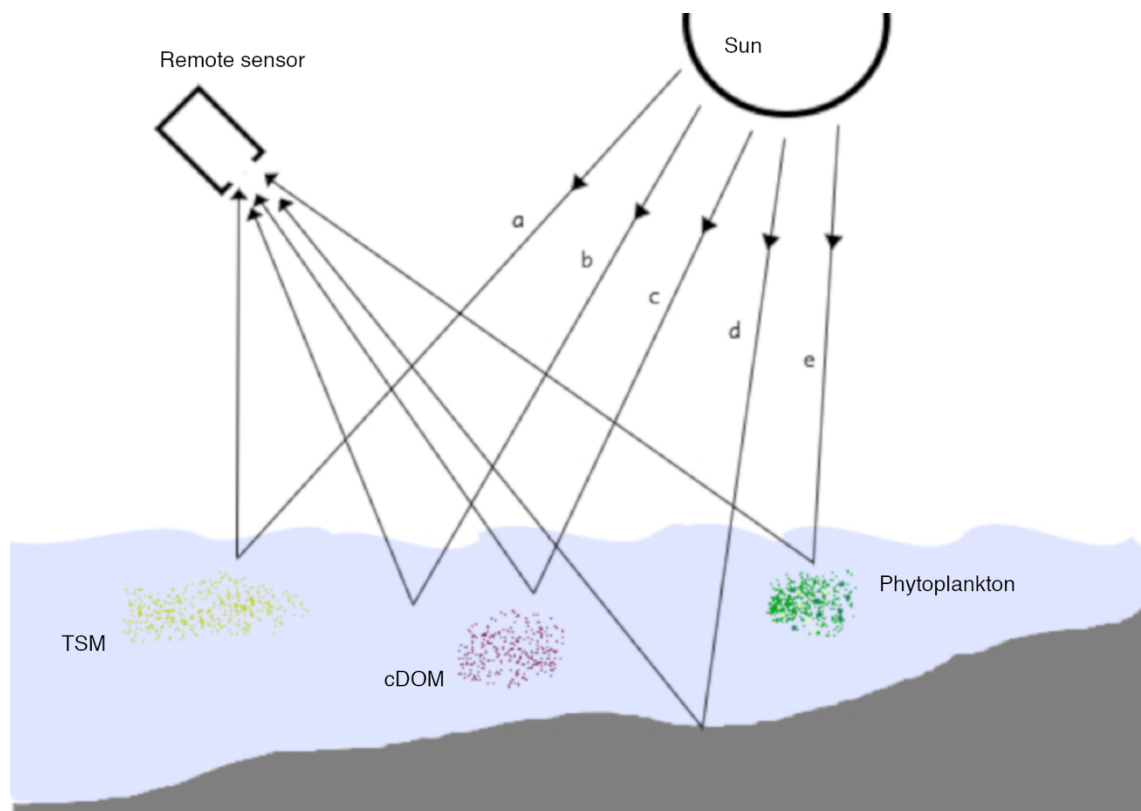
Figure 1.4: Different pathways of spectral irradiance is it travels to reach a remote sensor, and the factors that influence upwelling light leaving the sea surface. Including a) upward scattering by total suspended matter (TSM); b) upward scattering from water molecules; c) absorption of blue light and scattering by colored dissolved organic matter (cDOM); d) reflection from the bottom; and e) absorption of red and blue light, and scattering by phytoplankton components (Chl-a). The levels of these constituents (IOP) in the water will influence ocean color and the information that can be retrieved from images taken of the water masses (IOCCG 2000).

1.5. Experimental aims

There is potential for using instrument carrying mobile platforms (bio-drones, UAVs, ROVs) for detecting, tracking, counting, mapping and monitoring seabirds such as shags and their foraging habitat in order to indicate ecosystem health. Before this technology can be used for conclusive assertions, it must be tested for proof-of-concept. To improve the use of drones for data collection on the foraging behavior of shags this study will evaluate the advantages and shortcomings of using a combination of bio-, aerial-, underwater-drones to explore the foraging ecology of breeding European shags (*Phalacrocorax aristotelis,* Linnaeus 1761) based on experiences gained at the test site Runde, Norway (62.4006 N, 5.6242 E).

A pilot study was carried out with shags as bio-drones, as well as an aerial drone (UAV) and an underwater drone, miniROV (further denoted as ROV) operating simultaneously to provide surveys in areas of shag diving activity as identified by the bio-drones. The methods used during this study were adjusted and optimized through trial and error, using the experiences gained to take the next steps in the project in accordance with Nilssen et al. (2015). An additional study of the UAV's ability to identify OOI in the water column was done in the Trondheimsfjord (63.441091 N, 10.348245 E). The effect of weather and ocean conditions (e.g. waves, water transparency, solar illumination and cloud cover) on AOP in this study describe the parameters for evaluating advantages and challenges during this particular study and need to be re-evaluated before future work using drones under different optical conditions.

Using the European shag population breeding at Runde as a case study, this thesis aims to (1) explore the utility of shags as bio-drones to provide information on important foraging habitats, (2) evaluate an aerial drone's capacity for observing shag foraging behaviour, and its ability to identify objects of interest in the water column, as well as describing the effects optical properties of water have on UAV-based imaging, and (3) assess the utility of combining bio-, aerial-, and underwater drones to provide more information on important foraging habitats using shags as indicator species.

2. Methods

The procedures used in this thesis employ three different instrument carrying mobile platforms; the shags equipped with bio-loggers as bio-drones, the UAV as an aerial drone, and the ROV as an underwater drone. All three platforms were deployed in a field study between the 14th-27th of June 2017 during the breeding period of the shags. During the field work all three technologies were evaluated as independent technologies in studying shag foraging behavior, but an assessment was also made on the utility of using them together to map shag foraging behavior. A further test of the UAV was completed in Trondheim, 31st of August 2018, to evaluate the effect of IOP on UAV image quality as a function of depth and distance.

2.1. Study site

The field study was conducted on the island of Runde (62.4006 N, 5.6242 E) and the surrounding waters (Fig. 2.1). The birdlife on Runde is protected by the Goksøyr Mires Nature Reserve, and has historically been famous for the amount of seabirds inhabiting it (Barrett, Lorentsen & Anker-Nilssen 2006). The Norwegian Coastal Current and the North Atlantic Current (i.e. gulf stream) converge near Runde, and it is an important spawning area for fish, especially herring *Clupea harengus* (Andersen et al. 2009). Small-scale fishing and kelp trawling takes place within close vicinity of Runde, there is also fish aquaculture to the east of the island (Andersen et al. 2009).

Figure 2.1: Location of the Runde study site on western coast of Norway. The surveys areas are indicated by the red shapes. The shag colony on Runde is indicated by the white bird within a green circle. The first survey was completed south-west of Remøya, where shag diving activity was recorded. The second was at Kaldekloven, west of Runde, in an area with very little shag diving activity (MapTiler 2019).

2.2. Study species

The European shag (hereafter shag; Fig. 2.2) is a coastal bird species with a wide distribution in the northeastern Atlantic Ocean and Mediterranean Sea basin. Shags are important top-predators in many coastal systems, and is a near-shore forager that pursuit-dives for prey in kelp, sandy-bottom and pelagic habitats depending on season, location, and prey abundance (Watanuki et al. 2008; Hillersøy & Lorentsen 2012; Christensen-Dalsgaard et al. 2017). Since 1975, the population of breeding shags on Runde has suffered a decline of ~96% from 5000 pairs to no more than 200 pairs during the breeding season of 2017 (Barrett, Lorentsen & Anker-Nilssen 2006; Christensen-Dalsgaard 2018, personal communication, 15th of May). This makes it part of

the global trend of decreasing shag populations (IUCN 2018), though despite the local population decline at Runde, the shag population has remained steady and even increased in other parts of Norway making its overall status as of least concern in this country (NBIC 2019).
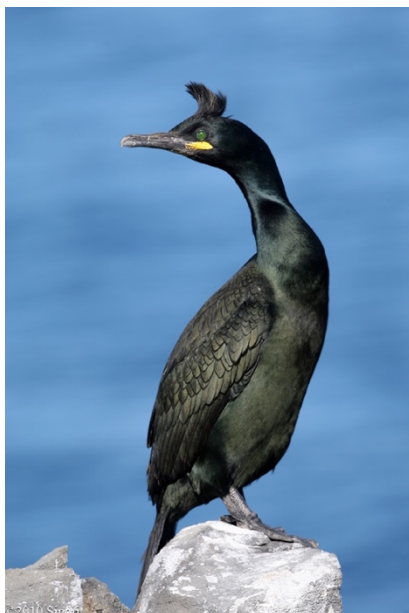
Figure 2.1: A European shag during mating season. Both males and females display a crest during the mating season, however it is gradually lost once the season is over (Sindri Skúlason 2010).

Along the Norwegian coast, gadoid species of fish and sandeels (Ammodytidae) have been found to comprise the majority of shag diets and are especially important during the breeding season (Barrett & Furness 1990; Swann, Harris & Alton 2008; Hillersøy & Lorentsen 2012; Bustnes et al. 2013). Full-grown shags regularly regurgitate pellets containing indigestible prey remains like otoliths or hard parts of Mollusca and Annelida, which can be collected and analyzed to identify what the shags are eating (Howell et al. 2018). Although they display dietary preferences, shags are able to alter their behavior according to variations in habitat or season, and such changes may reflect variations in the distribution and/or abundance of prey on a spatiotemporal scale (Barrett & Furness 1990; Watanuki et al. 2008). Because of their adaptability, shags and their dietary choices have been studied for use as indicators of ecosystem health and were found successful (Bustnes et al. 2013; Fortin et al. 2013; Lorentsen, Anker-Nilssen & Erikstad 2018). As such, this species has been recognized as having potential as a reliable indicator species, and is being considered as a sentinel of the state of the marine environment (Cairns 1988; Frederiksen, Mavor & Wanless 2007; Soanes et al. 2014).

2.3. Deployment of bio-drones and analysis of data

During the field study, the shags were used as bio-drones to map foraging behavior and habitat use with a logger unit comprised of a Geographic Positioning System loggers (GPS; logger type: i-gotU GT-120, Mobile Action Technology) and a Time Depth Recorder (TDR; G5, CEFAS Technology). The GPS- and TDR-loggers (from here on, logger units) were deployed to track shag diving locations, as well as the depth to which the shags dived. The maximum weight of deployment for the logger units was 30.6g. The logger unit was attached to the upside of 3-4 middle tail feathers of 19 shags using a zip tie and TESA® tape. Of these, 7 were recovered by recapturing the birds in their nests after 2-3 days to remove the logger units. Deployment of the loggers required about five minutes of handling per bird, while retrieval took on average six minutes.

The data retrieved from the bio-drone logger units were exported to Microsoft Excel 2016. The GPS-loggers were configured to record a position every 30 seconds, while the TDR-loggers recorded pressure and temperature every second following Christensen-Dalsgaard et al. (2017). The GPS location data were coupled with TDR-logger information to identify foraging areas within the shags' range. This data was then used to create a map of the shags' diving locations over a sediment map provided by the Geological Survey of Norway (NGU). The sediment map shows the distribution of sand, silt, boulder, and bedrock on the seafloor surrounding Runde and the nearby islands. The bio-drones were the first of the three mobile platforms to be deployed, and were sent out a for a week prior to the other two platforms (UAV and ROV) since the locations of shag diving activity determined the survey areas for the other two drones.

In addition to the data from the logger units, fresh regurgitations (< one day old) were collected from nearby the nests or on the rocks where the shags could be seen resting. The undigested otoliths in the regurgitated pellet samples (as well as any other undigested objects such as snail shells, polychaeta structures etc.) were measured and sorted by species to determine shag diet composition during the study period (Hillersøy & Lorentsen 2012; WoRMS 2019). Some otoliths were too small for identification (< 3 mm) further than Gadidae indetermined (indet.) and were classified as saithe[1] (Hillersøy & Lorentsen 2012). From the size of the otoliths found in the diet, the average length of fish was calculated using the equations from Härkonen (1986), and Jobling and Breiby (1986). From

---

[1] Analyses of the otoliths from diet samples were done by Grethe Hillersøy, and the back-calculations from otolith to fish size were done by Jørgen Strømsholm.

the fish length and knowledge on fish ecology, the habitat of the fish in the shags' diet could be identified, giving an indication as to the type of habitats the shags of Runde are foraging in.

2.4. UAV surveys and assessment

The UAV used in this study was a quadcopter drone of the type Phantom 4 SZ (DJI Technology Co., China; Fig. 2.3). The drone has a mass of 1380 g (battery and propellers included) and a diagonal length of 350 mm without propellers. The camera sensor mounted on the UAV's underside has a 1/2.3" complementary metal-oxide-semiconductor (CMOS) sensor, a Field of View (FoV) of 94°, 20mm lens, and provides video in 4K (3840x2160 pixels). The video footage in MOV format from the UAV was exported to a MacBook Air (Apple INC, USA) using a ScanDisk (U.S.A.) 32 GB micro SD memory card for processing.

Figure 2.3: DJI phantom 4 drone quadcopter used in this study. The drone has a mass of 1380 g (battery and propellers included) and a diagonal length of 350 mm without propellers. The camera hangs on the underside of the drone.

Two surveys were conducted near Runde with the UAV. Because of poor weather (strong winds and rain, Appendix 1), there were limited opportunities for UAV deployment, so the two surveys were therefore completed on the same day (23rd June, 2017). The first survey was in an area of known shag diving activity south of Remøya (62.359236 N, 5.618349 E). The second was by Kaldekloven (62.399874 N, 5.593619 E), a landmark on Runde near the shag colony where no diving activity was

registered (Fig. 2.1). While surveying these areas, the UAV looked for objects of interest (OOI) including seafloor substrate types and shag behaviors both below and above the sea surface. Because of the exploratory nature of the investigation, Nilssen et al. (2015) was used as a guide for the survey methodology and the data were analyzed to find images that best demonstrate any advantages and limitations of using the UAV in the marine environment.

2.4.1 Effect of IOP on image quality as a function of depth and distance

To obtain a better understanding of how the optical properties of water influence UAV image quality, a second study was done to evaluate image quality as a function of UAV elevation and ROV depth. The experiment was carried out at Trondheim Biological Station (TBS, Norwegian University of Science and Technology (NTNU), Trondheim) using Secchi disks mounted on the dorsal side of the ROV (Fig. 2.4). The ROV was submerged to 0, 1, 2, 3, and 5m depth, while the UAV flew above it at a 90° angle, taking pictures at 5, 10, and 30m elevation above the ocean surface.
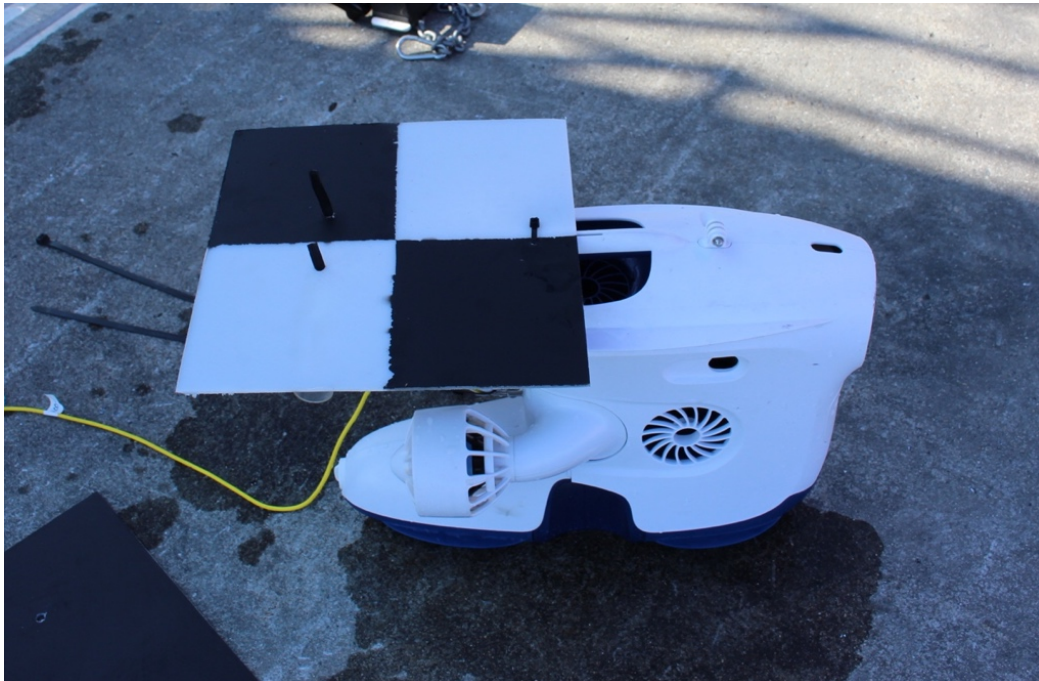
Figure 2.4: BluEye ROV with black & white Secchi disk attached to the top. The ROV was submerged to depths of 0m, 1m, 2m, 3m, and 5m with the disks mounted to assess the range of UAV camera sensor under the AOP conditions at the time of the study.

A Secchi disk is a device used to measure the transparency of sea water (Preisendorfer 1986). It is usually white, but often a black & white disk can be used as the pattern provides a better contrast

against the surroundings in sediment or plankton-rich waters (Sakshaug, Johnsen & Volent 2009). This method for measuring downwelling irradiance illustrates how far down into the water column an object can be seen by an RGB sensor (the human eye). A set of custom made Secchi disks of 30x30 cm were attached to a ROV (Fig. 2.5). The first Secchi disk was painted in a black & white checker-board pattern as a standard Secchi disk for reference. The second was painted with a light brown color to look like sea floor sand (RGB # 252, 226, 201). Bladder wrack (*Fucus vesiculosus*), mimicking the color of brown macroalgae (including kelp) was laid and secured with thin twine on top to prevent the wrack from floating when submerged. The final disk was all black to emulate the shag as an OOI beneath the sea surface. The plastic used to make the Secchi disks was white polyethylene, so only black paint (RGB # 38, 38, 38) was needed for the black & white and black Secchi disks.

Figure 2.5: Color pattern of three Secchi disks used in study. The left Secchi disk is a standard black & white, used in most Secchi depth readings. The middle Secchi is painted to mimic a sandy substrate overlaid with wrack to imitate kelp forests. The final disk is painted black to imitate a shag under water.

To determine the IOP of the water during the UAV study at TBS, an ECO triplet (Wet Labs, USA) was used to measure concentration of Chl-a (as a proxy for phytoplankton biomass), cDOM, and TSM according to Fossum et al. (2019). The sampling took seven minutes, as the instrument was held at each depth (1, 2, 3, and 5m) for ~1 minute to stabilize, with four samples taken per second (4 Hz). Knowing the IOP levels at the time of the study aids in the interpretation of changes in the color and contrast of the OOI seen in UAV images. It also provides references for future studies as to what effects the IOP conditions have on the visibility of an OOI under the conditions of this experiment.

2.4.2. Measuring effect of IOP on image quality

To quantify the effect of the IOP on image quality, the images taken by the UAV were processed using GIMP (GNU Image Manipulation Program) (GNU GPL v3+, 2018, GNU). In order to only include the Secchi disks in the analysis and no other parts of the image like the ROV, solar glints or the surrounding waters, the images were cropped (Fig 2.6.A) so that the Secchi disk filled as much of the frame as possible. In the analysis, only one color was sampled at a time to prevent color mixing skewing the RGB color values. To do so, an opaque frame was fitted over the image, leaving a transparent area over the color of interest (2.5.B and 2.5.C). The RGB color sampling only took samples from within the transparent area of the image. For example, when analyzing the RGB values for the sand-colored part of the Secchi disk, the opaque layer (Fig. 2.6.B.) hid all parts of the image that were not the sand colored part of the disk. When sampling RGB values from the kelp-colored part of the same image, the old opaque layer was removed (returning the image to Fig. 2.6.A) and a new layer was added so that only the kelp color was visible through the layer (Fig 2.6.C).
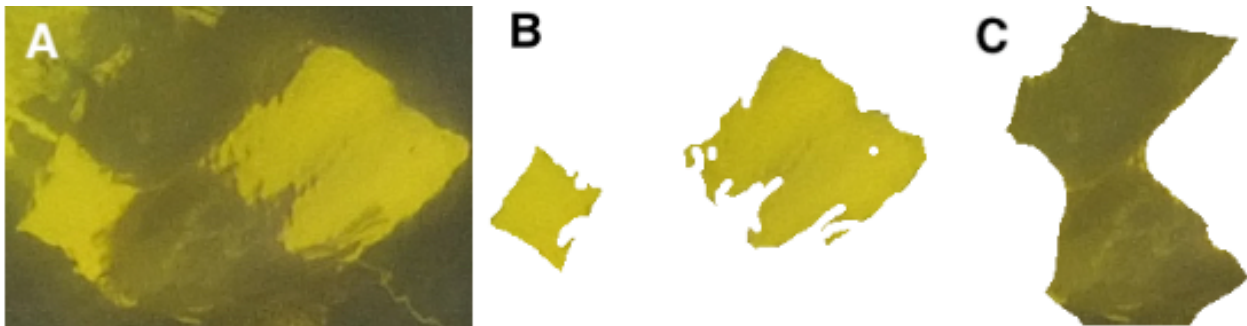

Figure 2.6: Method for preparing Secchi disk images for RGB color determination by adding an opaque layer to the image. Only one color is visible through the transparent layer, so RGB value analysis is only done of one color at a time. (A) shows the whole kelp & sand colored Secchi disk, as well as parts of the ROV, its umbilical, and surrounding waters. After the first round of processing, the image (B) shows only the sand color of the Secchi disk. In (C) only the *Fucus vesiculosus* on the Secchi disk can be seen, so that the average RGB value of the kelp colored part of the Secchi disk can be found. This method prevents colors from being mixed, and prevents the inclusion of other objects (ROV, umbilical, solar glints) in the analysis. Despite the selection process, wave action and the angle of light still cause color variation, which is why the average of 50 pixels was taken for each color to prevent bias in the RGB values. The aerial drone is at 5m elevation, the ROV at 2m depth.

To avoid selection bias in the RGB color analysis, 50 pixels were randomly chosen and averaged for each color within the transparent layer. The process was accomplished using a custom script in Clojure (2007), programmed to select 50 pixels in the transparent area of an image. The value

of each of the 50 samples for each image (Appendix 3) was exported to Excel (Microsoft Corp. U.S.A.) for further processing of color information.

2.5. BluEye drone (ROV)

For the underwater photography taken at Runde, an underwater drone (ROV) from BluEye (Norway) was operated where the logger units from the bio-drones indicated the shags were foraging. The ROV was used to map substrate types and depths, and to document the species and size of fish (or other organisms) seen along the transects. During the surveys, the ROV and aerial drone were coordinated and used simultaneously so that the pilots could provide each other with information such as location, substrate, and objects or areas of interest. As this thesis places emphasis on the bio-drones, the UAV and on assessing the use the three drones (bio- aerial, and underwater) together, the technical specifics and methodology used for the ROV will not be listed here. Instead, the data analysis methodology and an in-depth review of the results from the ROV can be found in Strømsholm (2018).

3. Results

The bio-drones in the study provided sufficient data to determine important foraging areas for the shags at the time of the observation (Fig. 3.1). The UAV was able to identify the location of islets and shallow kelp forest growth in the survey areas (Fig. 3.7-Fig. 3.9), but was limited by color change in the OOI and the specular reflection on the ocean surface both in the field and in the Trondheimsfjord, despite the AOP conditions being different in the two locations. The ROV mapped substrate types in the survey area (Fig. 3.12), and was also able to identify fish species and count them from the ROV footage (Fig. 3.11).

3.1. Bio-drones

The bio-drones provided a comprehensive insight into the foraging behavior of shags at Runde at the time of the study, and when combined, the two sources of data (logger units and diet samples) resulted in an extensive overview of both foraging locations and dietary choices.

3.1.1. Results from logger units on bio-drones

From the logger units deployed, a total of 861 diving locations were registered (Fig. 3.1). The shags foraging trips were between 200m and 13km in length, with an average trip length of 4.65km ($\pm$ 9.18). Only 0.02% of recorded dives were near the colony at Runde. Although all were within a close range of Runde, the diving locations were spread out fairly evenly across the range (Appendix 5). The mean diving depth of the shags was shallow at 19.9m, with maximum of 41.5m ($\pm$ 2.13).
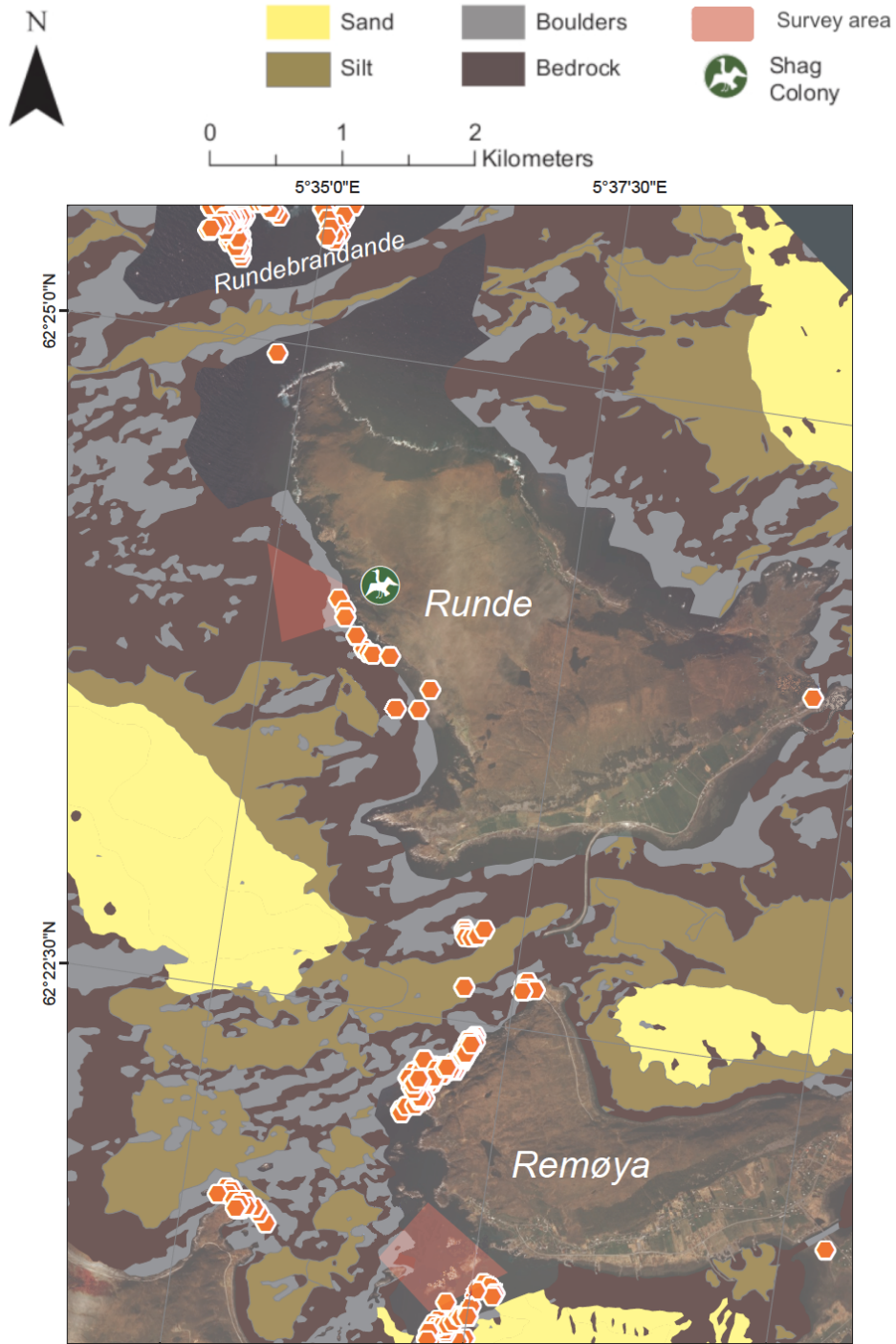
Figure 3.1: Sediment map with GPS positions of diving locations (n=861) showing substrate types in areas where shags were diving. The locations were mapped using the logger units deployed with the bio-drones. The UAV surveys and ROV transects were completed within the red shapes. The shag colony is indicated by the green bird on the north-west coast of Runde. No shags dove to the north-east of Runde, and Rundebrandane to the north of the colony was most frequented with 23% of total dives (NGU 2019).

The location with the highest diving activity (~23% of total dives recorded) was Rundebrandane (62.25328 N, 5.34462 E; Fig. 2.1), an area of low-tide elevation (land submerged at high-tide). The sediment map shows that the shag diving locations around Runde and Rundebrandane were dominated by hard substrates of bedrock and boulder, while locations to the east and south of Remøya were mainly above soft substrates like sand and silt (Fig. 3.1). No shag dives were recorded diving to the north-east of Runde during the study period. The sediment map from NGU does not cover the full range of shag diving locations, but another map with all diving locations (but no sediment types) was also created (Appendix 5).

3.1.2. Otoliths in regurgitated diet pellets from shags

Analysis of the regurgitated diet pellets collected from shags at Runde found nine different families of fish and a total of 13 species in the pellets (Table 3.1). Hard structures belonging to organisms within the subphylum Crustacea were found, but could not be identified to species level. Similarly, mandible structures from class Polychaeta could not be identified further. In addition to the organisms listed, 170 otoliths could not be identified further than the class Pisces and were therefore not included.

Table 3.1: Overview of prey species found with otolith analysis of regurgitated pellets from shag. The total number of individuals found in the diet samples was n=1415. A total of 13 species of fish were identified from the otoliths. Other structures such as parts of crustacean's shells or the mandible of Polychaeta could not be distinguished to species level.

Family	English common name	Number of individuals, (% diet by ind.)	Norwegian common name	Latin name	Associated habitat type
Ammodytidae	Sand lance	99 (6.99%)	Sil/Tobis	*Ammodytidae* (Bonaparte, 1832)	Sandy bottom
Cottidae *Total = 60*	Longspined bullhead	59 (4.16%)	Dvergulke	*Taurulus bulbalis* (Gratzianov, 1907)	Kelp forests and shallow reefs
	Cottidae indet.	1 (0.07%)	Ulkefamilien		Kelp forests and shallow reefs
Gadidae *Total = 938*	Atlantic cod	41 (2.89%)	Torsk	*Gadus morhua* (Linneus, 1758)	Kelp forest (while juvenile)
	Pollack	24 (1.69%)	Lyr	*Pollachius pollachius* (Linneus, 1758)	Kelp forest (while juvenile)
	Poor cod	249 (17.59%)	Sypike	*Trisopterus minutus* (Linneus, 1758)	Muddy or sandy bottom

	Shore rockling	7 (0.49%)	Tangbrosme	*Gaidropsarus mediterraneus* (Linneus, 1758)	Hard bottom
	Saithe	62 (4.38%)	Sei	*Pollachius virens* (Linneus, 1758)	Kelp forests (while juvenile)
	Tadpole fish	1 (0.07%)	Paddetorsk	*Raniceps raninus* (Linneus, 1758)	Kelp forest, eelgrass, and hard bottom
	Gadidae indet.	554 (39.15%)			Kelp forests (while juveile)
Gobiidae	Black goby	1 (0.07%)	Svartkutling	*Gobius niger* (Linneus, 1758)	Sandy or muddy bottoms, seagrass or seaweed.
Labridae *Total = 287*	Cuckoo wrasse	3 (0.21%)	Blåstål	*Labrus mixtus* (Linneus, 1758)	Kelp forests
	Corkwing wrasse	8 (0.56%)	Grønngylt	*Symphodus melops* (Linneus, 1758)	Shallow rocky sea bed among algae and kelp
	Goldsinny wrasse	10 (0.71%)	Bergnebb	*Ctenolabrus rupestris* (Linneus, 1758)	Seaweed and kelp forests
	Wrasse indet.	266 (18.79%)		(G. Cuvier, 1816)	Kelp forests, seaweed, rocky bottom among algae
Lottidae	Common ling	6 (0.42%)	Tangbrosme	*Molva molva* (Linneus, 1758)	Rocky substrate
Crustacea (subphylum)		3 (0.21%)	Krepsdyr	(Cuvier 1795)	
Pholidae	Rock gunnel	4 (0.28%)	Tangsprell	*Pholis gunnel* (Linneus, 1758)	Kelp forests and rocky bottom
Pleuronectidae	Flatfish	8 (0.56%)		(Linneus, 1758)	
Polychaeta (Class)	Bristle worms	4 (0.28%)	Flerbørstemark	(Grube, 1850)	
Zoarcidae	Viviparous eelpout	5 (0.35%)	Ålekvabbe	*Zoarces viviparus* (Linneus, 1758)	Kelp forests and rocky bottom

The pellet samples from Runde indicate that the shags foraged mostly on Gadidae (n=938), which made up 66.2% of the identified fish otoliths. Labridae (n=287) comprised a significant amount of the total species composition in the diet samples, contributing to 20.2% of diet composition. The most abundant species was poor cod of which a total of 249 individuals could be found in the pellets, meaning this species alone comprised 17.6% of the shags' diet. The variety of family, phylum, and class is quite wide, and the fraction of other (i.e. non-gadoid or sandeel species) is quite high at 26,2% of total identified otoliths.

From the otoliths in the shag diet, fish length was calculated. The average length of gadoid fish found was 117.18 mm, for labridae it was 136.66mm, while the average fish size overall was 96.49 mm The findings show that 24.66% of the species identified from otoliths were associated with sandy or muddy bottom habitats, 73.35% were associated with the kelp forest (some can also be found amongst cobble and rocky bottom sheltered by algae), and the remaining 1.99% could not be associated with a habitat due to the lack of information.

3.2. Field surveys and influences on image quality

When using UAV-based imaging to identify OOI in the water column, changes in object color and decreases in upwelling light influence visibility of the OOI (Fig. 3.3 and Fig. 3.7-Fig. 3.9). Increased distance to the OOI decrease both spatial resolution and color intensity (Table 3.8, Fig. 3.10), making accurate identification of OOI more difficult as depth increases, though the degree of the effect will depend on AOP conditions at the time.

3.2.1. UAV survey of objects of interest above the sea surface

The UAV was able to detect OOI above the sea surface and managed to get within the range of shags and other seabirds. No shags were seen while foraging nor while resting at the sea surface. While flying the Remøya survey, two shags were seen along with two great black-backed gulls (*Larus marinus,* Linnaeeus, 1758) sitting on an islet (Fig. 3.2). The presence of guano covering the rock suggests that shags rest here regularly.

Figure 3.2: UAV image of two shags and two great black-backed gulls on an islet during the survey by Remøya. Some guano (white stripes) on the rock indicates the shags rest here regularly. Spatial resolution 891x414 pixels.

While mapping the shag nesting area (65.400054 N, 5.596485 E) during the Kaldekloven survey (Fig. 3.1), a shag flying towards the colony was captured by the UAV camera (Fig. 3.3). The speed of the shag made it impossible for the UAV to follow its flight, and the shag was only in the field of view for a moment.

Figure 3.3: UAV image of shag in flight above nesting area. While flying a survey along the shag colony on the South West coast of Runde, a shag (within the white circle) in flight back to the colony was spotted. Known nesting areas of shags are identified with white arrows. Spatial resolution 2560x1440 pixels.

Also during the Kaldekloven survey (Fig. 3.1), several shags could be seen resting on a large rock (Fig. 3.4). The rock was probably a popular resting site, given the amount of guano covering it. There were also 100+ puffins (*Fratercula arctica*, Linnaeus 1758) and common guillemots (*Uria aalge,* Pontoppidan 1763) observable at the sea surface in this area (Fig. 3.5) near the shag resting area (Fig. 3.4).

Figure 3.4: UAV photo of shags resting on a large rock near the nesting site. Shags could often be spotted on this stone drying their wings, or just resting during the field study. The amount of guano (white) covering the stone suggests the birds spend a lot of time here, as do the GPS data. Spatial resolution 1038x688 pixels.

Figure 3.5: Puffins and common guillemots at sea surface near Kaldekloven observed with UAV. The birds appeared wary of the drone, and would quickly dive if it was too close (within ca. 15m). Spatial resolution 932x763 pixels.

3.2.2. UAV survey near Remøya

From the bio-drone data, the survey area south of Remøya (Fig. 3.1) was a known area of shag diving activity. During the survey, the water surface was highly reflective, creating a high ratio, approximately 25-100%, of specular reflection (glare) in the images which resulted in decreased visibility for any objects beneath the surface. The glare from the surface prevented information on OOI such as the ROV location from reaching the UAV sensor, but when the UAV changed its position to a different angle relative to the sun, the light field changed so that the ROV at 2-3m depth was detectable (Fig. 3.6).

Figure 3.6: Effect of solar reflection and sensor angle on image quality. The images were taken at ca. 15m (left) and 10m (right) UAV height. The difference in sun direction and waves affected the AOPs at sea surface. Here, glare caused by specular reflection hinders information from beneath the water surface from reaching the sensor (left). The ROV is within the white circle, but because of the camera angle in relation to the sun and the resulting glare it cannot be identified. When the angle of the camera in relation to the sun and OOI, the ROV can be detected at ≈3 m depth.

The occurrence of specular reflection was higher while flying with the UAV sensor straight above (at a 90°) to the object. When the angle in relation to the sun and the OOI was changed during the survey, it altered the light field so that substrate types and the ROV could be seen despite a distance of nearly 200m to the object and 50m elevation (Fig. 3.7). The red-brown kelp forests could be distinguished from the sandy substrate when looking at the survey area from an acute angle rather than perpendicularly, creating an overview of the environment the ROV was transecting. The kelp forests could only be identified with certainty above 4m depth under the AOP conditions of the survey, while sand was easily seen as light green regions. The contrast in color made it possible to see where there was kelp or sandy substrates, but glare still limited image quality in the upper quarter of the image.
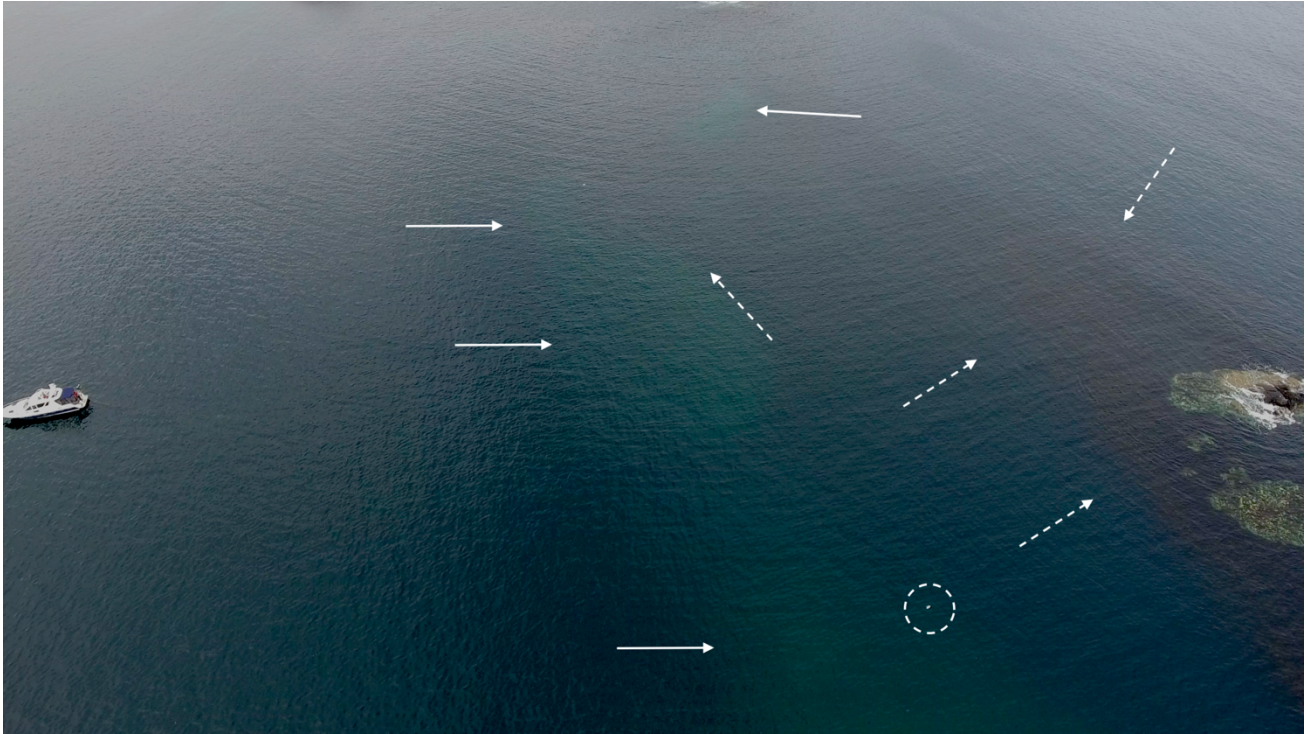
Figure 3.7: UAV image from Remøya mapping ROV transect direction, kelp growth, and sandy seafloor. At this camera angle, the ROV (indicated by the white circle) is clearly visible, as it has surfaced from a transect despite the distance from the UAV. In addition, the different types of subsea habitats can be quite clearly discerned. The areas covered in kelp (red-brown to dark brown, indicated by dashed white arrows) are easily differentiated from the sand (light green, indicated by white arrows) in the middle of the image. Spatial resolution 2560x1440 pixels.

3.2.3. UAV survey at Kaldekloven

During the drone survey at Kaldekloven and the shag colony (Fig. 2.1), the sky was overcast, again creating an optical environment with a high ratio of specular reflection (Appendix 1). There were very few shag dives recorded in the area, in spite of its proximity to the nesting area and kelp forest growth. Despite the specular reflection, the UAV captured images where areas of kelp could be identified (Fig. 3.8), and both the ROV and its umbilical could be seen throughout the transect (Fig. 3.9).

Figure 3.8: Tracking the ROV with the UAV during the Kaldekloven transect. At ~10m UAV elevation, the level of detail in the image is quite high. Details of the ROV, such as its shape are easily recognizable. Also, structures of individual kelp lamina to the ROV's left can be seen in the image. What appears to be kelp growth can also be identified with the UAV at this height, but the effect of IOP make it less certain as depth increases. Spatial resolution 2560x1440 pixels.

The UAV could detect kelp growth to a depth of about 5m, and when flying at low elevations (5-10m) details of kelp lamina could be seen in the UAV images (Fig. 3.8). At ocean depths beneath 5m, the kelp lost its red-brown color and became indistinguishable from the surrounding water. Even from altitudes above 60m, the ROV was clearly visible because of the low IOP concentrations in the water (Fig. 3.9). During this survey, the UAV mapped upper layers of kelp growth with success and could easily outline the location of islets along the transect, yet could not identify the sandy substrate at 19-23m depth found by the ROV.
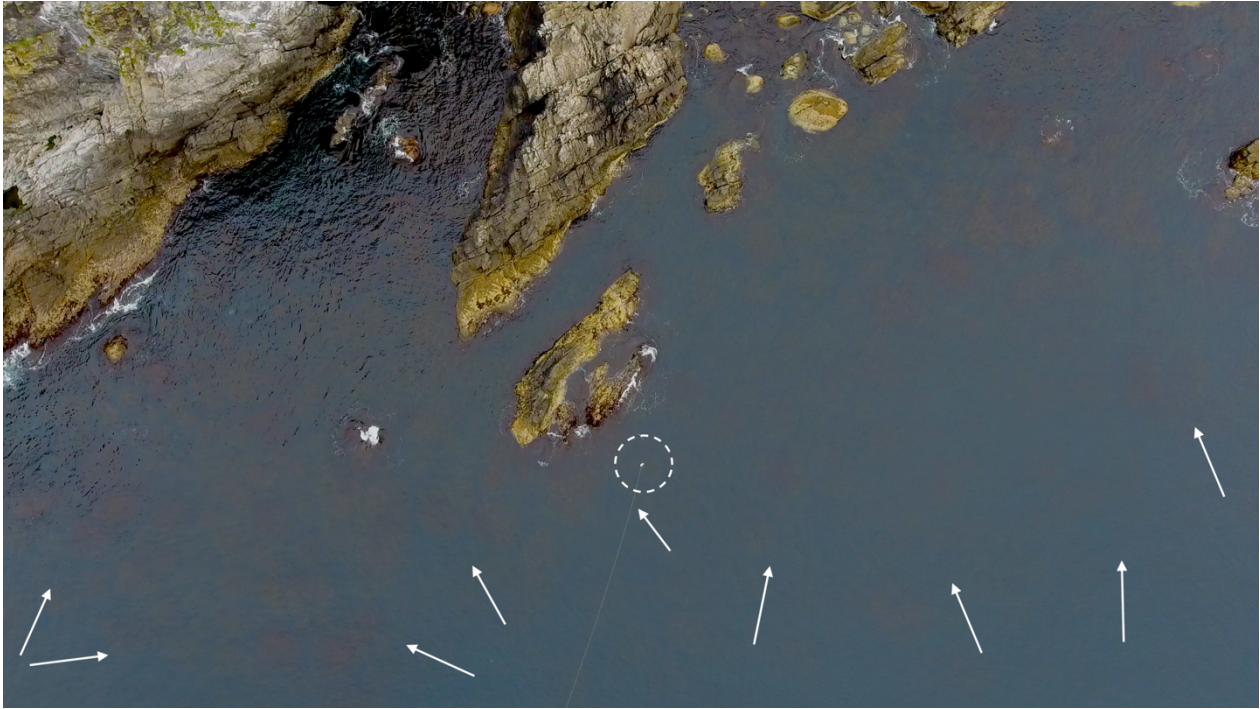
Figure 3.9: UAV image of kelp growth and ROV transecting waters near shag colony at Kaldekloven from 60m altitude. The kelp forest in the area (indicated by white arrows) can be seen as red-brown regions. No other types of substrates can be identified from this image. Because of the light conditions at this moment, the ROV (dashed white circle) and its umbilical cord (dashed white arrow) can be easily discerned. Screen shot from UAV footage. Spatial resolution 2560x1440 pixels.

3.2.4. Image quality and the effect of the Inherent Optical Properties of water

The study of UAV image quality as a function of UAV elevation and ROV depth found that as distance increased between OOI and UAV sensor, the spatial resolution of the image decreased (Fig. 3.10), as did color intensity (Table 3.3). In addition, increasing depth of the OOI also caused a distortion of OOI shape (Table 3.9). IOP in the water masses have a larger effect on image quality as depth increases, and are highly affected by the ratio of Chl-a, cDOM, and TSM in the water. The average IOP concentrations measured with the ECO triplet sensor during the assessment indicated medium phytoplankton biomass in the water masses, low TSM levels, and mid to high values of cDOM (Table 3.2).

Table 3.2: Average ECO triplet-derived values (n=1745) for TSM, Chl-a, and cDOM measured in concert with Secchi disk on ROV images. These values give an indication of the IOP of the ocean at this moment in time, thus supporting an explanation for the reduced visibility and color change seen during the study.

	Average	Max	Min
TSM (m^{-1})	0.0017	0.0131	0
Chl-a (µgL^{-1})	1.572	15.1402	0
CDOM (ppb)	0.475	36.162	0

Both from the UAV images of the Secchi disk (Table 3.9) and from the average RGB values (Appendix 2), it became apparent that the cDOM levels in the water masses caused an increase in the yellow color of the OOI as depth increased. This was especially visible for the lighter colors (white and sand; Table 3.5 and 3.7), whereas the darker colors (black and kelp) appeared more green due to the mixing of the dark color and yellow (Table 3.4, 3.6, and 3.8). At 3m depth, the colors all appear green because of the effect of IOP, making it impossible to determine the original color of the disk (Table 3.3).

Table 3.3: Overall trends of color change found in Secchi trials in the Trondheimsfjord, showing effect of IOP on color as a function of depth. The decrease in color saturation can be seen as UAV height increases from 5m to 30m. At 3m depth, the color of all the Secchi disks homogenizes to similar shades of green.

ROV Depth/UAV Height	Black (B&W)	White	Kelp	Sand	Black
Color at 0m/5m					
Color at 0m/30m					
Color at 3m/10m					

The black & white Secchi disk could be seen without difficulty until 3m depth at all altitudes, yet at 5m depth the visibility was greatly reduced. The contrast between the black and white colors aided in identifying the Secchi disk making it easier to detect, especially at 3 and 5m depth (Appendix 3).

Table 3.4: Darkening of the black part of black & white Secchi disk due to IOP as a function of ROV depth and UAV elevation. As Secchi depth increases, the black color gradually becomes more yellow, yet because of the mixing of colors it appears dark green already at 2m depth.
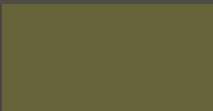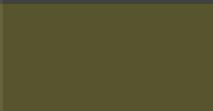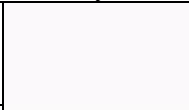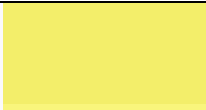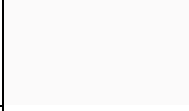
UAV elevation (m)					
30					
10					
5					
	Secchi depth (m)	0	1	2	3

Table 3.5: The yellow color caused by cDOM concentration is very clear for the white part of black & white Secchi disk. The color changes further towards dark green as a function of ROV depth and UAV elevation. At 3m depth the white color is very similar to the black colored part of the disk shown above.
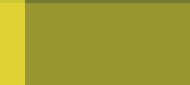
UAV elevation (m)					
30					
10					
5					
	Secchi depth (m)	0	1	2	3

UAV images of the kelp & sand colored Secchi disk had the highest visibility and could be identified for the whole range of heights and depths included in the trial (Table 3.9). The yellowing is also clear for this Secchi disk, as is the darkening at 3m depth. Furthermore, the red of the kelp at the sea surface shows a clear decrease in color saturation at higher UAV elevations (Table 3.6).

Table 3.6: The red color of kelp becomes green already at 1m ROV depth when cDOM concentrations are high. This disk had the highest visibility during the trials. As Seechi depth increases, the red of the wrack gradually becomes more yellow and green as ROV depth increases. The dark green color at 3m makes it hard to distinguish the kelp colored part of the Secchi disk from the lighter sand colored part. Also, the red color of the kelp lost saturation as UAV height increased even when Secchi depth was the same, so that the color as seen by the sensor was less intense.

UAV elevation (m)						
30						
10						
5						
Secchi depth (m)	0	1	2	3	5	

Table 3.7: With increasing Seechi depth, the light brown color mimicking sandy substrates gradually becomes more yellow before becoming green at 3m depth. The color at 5m ROV depth is indistinguishable from the kelp colored part, making it appear monochrome dark green.

UAV elevation (m)						
30						
10						
5						
Secchi depth (m)	0	1	2	3	5	
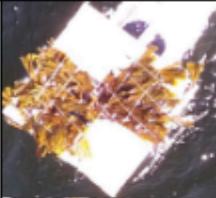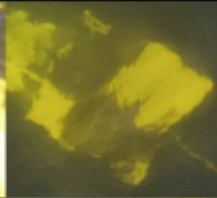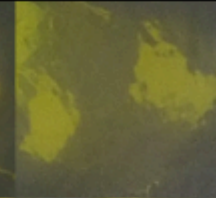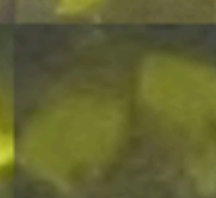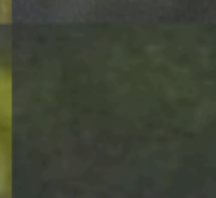
The black Secchi disk had the poorest visibility of the three Secchi disks. Already at 2m depth, the black disk could not be seen in the UAV images. However, identification of the disk was possible because of the white body of the ROV being visible. This revealed the black Sechhi disks location and the shape at 2 and 3m depth. The yellow gradient caused by IOP was also apparent for this Secchi disk, though it appeared more brown due to the mixing of black and yellow (Table 3.8).

Table 3.8: Color change in black Secchi disk as ROV depth and UAV elevation increases. The black color gradually becomes more yellow already at 1m depth, but the mixing of black and yellow makes it appear green. At 3m depth the color becomes darker green, similar to the color seen in the other Secchi disks at this depth.

UAV elevation (m)					
30					
10					
5					
	Secchi depth (m)	0	1	2	3

In addition to color change and darkening causing a homogenization of Secchi disk colors towards green, several influences on image quality coalesced to decrease visibility of the OOI. When the Secchi disk was at the sea surface, the turbulence it caused in the water caused an increase in solar glints to occur on its surface so that there were several overexposed points in the images (Table 3.9). Furthermore, the wave action changed the path of the light moving towards the UAV sensor, thereby distorting the shape of the Secchi and making it appear less square.

Table 3.9: The UAV images showing how IOP, depth of OOI, elevation of UAV, and light interact to change the color and shape of the OOI. The images are of kelp and sand colored Secchi disk (simulating kelp forest and sandy bottom substrates) mounted on ROV. This was the only Secchi that could be identified at all drone heights and ROV depths, mainly due to the contrast in color provided by the sand-colored parts of the Secchi disk. Note that at 2m depth and below the brown of the wrack was indistinguishable from the black Secchi disk when only looking at the images with the naked eye. Because of the increase in height of the aerial drone, the resolution of the images decreases with height, so at 5m elevation, resolution is 382 x 343 pixels, at 10m elevation 131 x 132 pixels, and at 30m 34 x34 pixels.

In addition to color change affecting image quality, the images' spatial resolution also decreased with increasing UAV sensor altitude. At 5m elevation the spatial resolution was 382x343 pixels, at 10m it was 131x132 pixels, while at 30m elevation, the resolution was quite poor at 34x34 pixels (Fig. 3.10). The exact spatial resolution varied between images, as they were cropped differently to best fit the Secchi disk (Appendix 4).

Figure 3.10: Decrease in spatial resolution of UAV images as elevation increases. The black & white Secchi disk is shown at the sea surface (0m depth), while the UAV flies at 5, 10, and 30m elevation. As height increases, the spatial resolution decreases from 382x343 pixels, to 131x132 pixels, to 34x34 pixels. Due to this effect, there is a lack of detail in the image at 30m and the OOI is very pixelated.

3.3. ROV information from beneath the surface

From Strømsholm (2018), it was found that the ROV was best able to identify fish of 100m or larger in size. The underwater drone was able to successfully explore both sheltered and exposed areas during the surveys, and mapped substrate type and depth during its transects.

The ROV transect at Remøya (Fig. 2.1) confirmed the presence of kelp forests of *Laminaria hyperborea* (Gunnerus 1766) from the littoral zone down to 18m depth. At further depths sand was the primary substrate until the maximum transect depth at 25m. There, the sandy sea floor was covered with fragments of detached kelp tissue and many gadoid fish were seen swimming over the debris (Fig. 3.11).
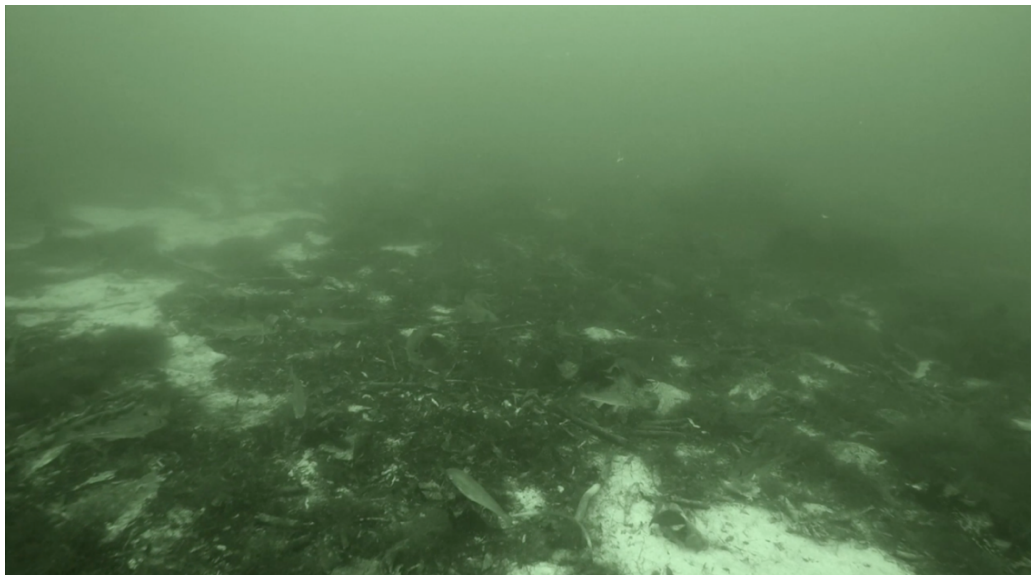
Figure 3.11: Sandy substrate at Remøya covered in macroalgal debris and gadoid fish swimming above. Image from ROV transect at 25m. Above 18m depth, the ROV found the substrate was dominatated by *L. hyperborea*. Spatial resolution 1428x798 pixels.

During the next survey at Kaldekloven (Fig. 2.1) the ROV found that the seafloor was mostly covered by kelp down to 19m depth (Fig. 3.12), with sand at 19-23m. The kelp was dominated by *L. hyperborea,* but *Saccharina latissima* (Linnaeus 1753) and *Alaria esculenta* (Linnaeus 1767) were also found. Few of the fish found in this transect were within the size range calculated from the otoliths found in the regurgitated shag pellets at the time of the study.

Figure 3.12: Kelp forest from Kaldekloven transect. The image from the ROV transect shows the area was dominated by *L. hyperborea*, but other kelp species like *S. latissima* and *A. esculenta* were also found. Few fish within the shag size range were seen in this area. Spatial resolution 1260x804 pixels.

4. Discussion

The bio-drones provided a broad insight into shag foraging behavior, and marked important marine areas for the aerial and underwater drones to explore (Fig. 3.1). The poor weather during the field work, including strong winds and rain, limited the window of opportunity for deployment of the UAV (Appendix 1). The two surveys at Remøya and Kaldekloven were therefore completed on the same day, so that the AOP observed in the field are similar for the UAV survey. At both Runde and TBS it was discovered that objects (including substrates) with colors contrasting to their surroundings could be detected by the UAV to further depths than objects without (Fig. 3.7; Table 3.4-3.8). Furthermore, image quality was highly variable depending on the light environment (Fig. 3.6), IOP concentrations (Table 3.2), and distance to the object (Fig. 3.10). The ROV was able to confirm the substrate types and species biodiversity in the survey area, providing *in situ* observations of the shags foraging habitat. The UAV provided no insight into foraging behavior, but when used with the ROV it provided information that allowed the ROV to perform its transect without losing its course or crashing into obstacles. The three drones together as an approach to seabird mapping and monitoring have potential for improving the amount of information in an indicator species study, but need to be assessed further before being used in decision-making.

4.1. Bio-drones to provide information on important foraging habitats

Using shags as bio-drones provided valuable information that could be used to determine important foraging areas for the shags and indicated important areas for their prey. The logger units and diet samples both provide comprehensive insight into aspects of shag foraging behavior and prey preferences. This not only hints at trends within the ecosystem, such as fish population recruitment (Lorentsen, Anker-Nilssen & Erikstad 2018), it also illustrates which areas and habitat types are important for the health of the local ecosystem.

Overall, 73.35% of the shags' diet was associated with the kelp or the rocky substrate beneath kelp, while 24.66% was associated with sandy or muddy bottom. It was found that the shags' diet was made up of 66.2% juvenile gadoid fish from six different species, with species of labridae being second most common (20.2%), both species groups are associated with kelp forests. Compared to other studies on shag diet, the findings at Runde show the shags here are eating a large portion of "other" species (Barrett & Furness 1990; Hillersøy & Lorentsen 2012; Bustnes et

al. 2013). In other locations, shag diets have been shown to be dominated by either saithe (Sklinna, 65.200898 N, 11.000044 E) or sandeel (Hornøya, 70.387739 N, 31.154167 E). With 26.2% of their diet being made up of other species than gadoids or sandeel, the shags at Runde seem to be making different choices compared to two other shag populations in Norway. Shags are known to be adaptable to changes in prey availability, so it is difficult to determine whether the large proportion of labrids is due to low availability of gadoids and sandeel or a high abundance of labrids. Considering the dramatic decrease in the shag population in this area (96% since 1975), the diet choices could indicate that the shags are having trouble finding sufficient resources for recruitment and are having to choose different prey because of low recruitment among fish populations in the area.

The average length of gadoid fish found through back-calculation from otolith length was 117.18 mm (min. 20.33mm, max. 304.04mm), while the average fish length overall was 96.49mm (min. 20.33mm, max. 304.04mm; Appendix 4). A length of 117.18mm is within the juvenile size range for gadoids (40-153mm), which is also the life stage at which most species of Gadidae live in kelp forests (Fey & Linkowski 2006). As such, the fish length calculated from the otoliths identified kelp forests as important habitats since the shags were mainly eating juvenile gadoids and labrids associated with kelp. This method of using bio-drones may indicate relevant nursery areas for fish populations. This is particularly useful when using shags as indicators of important marine areas for fish recruitment, which is an important aspect of ecosystem health (Lorentsen, Anker-Nilssen & Erikstad 2018).

When combined with a current map of sediment/substrate types in the foraging area as the one used in this study (Fig. 3.1), the location and depth of the dive can give a clue as to the type of prey the shags may be targeting. For example, frequent diving activity in areas with kelp growth could therefore indicate that shags are foraging for gadoid fish. The sediment map shows that the substrate surrounding Runde was mainly hard bedrock and boulders, which are good conditions for kelp growth. Even though the logger units and sediment map are not conclusive when it comes to linking location and dietary choices for shags, they do stand to reason, though the use of the sediment map would have been improved by a map of kelp growth in the area.

According to the map of GPS-locations (Appendix 5), the shags did not travel far from the nesting area to forage, which was expected since it was the breeding season and they were limited

by distance to the nest (Christensen-Dalsgaard et al. 2017). The average distance traveled to a diving location was 4.95km, and the area most frequented was Rundebrandane (23% of total dives), which is about 3.5km away from the colony. Curiously, no shags dived to the east of Runde during the study period (Fig. 3.1 and Appendix 5). This region is an area where kelp trawling and fish aquaculture take place (Andersen et al. 2009), and it may be these industries are having negative effects on the local environment by destroying habitat, polluting the water masses, or both. There is a reason why the shags are choosing not to forage in this area and their decision could be a signal that the environment in this location is doing poorly, which would be an interesting topic for future studies of this shag population.

The weather provided a set of challenges when working with the shags as bio-drones. There were days of rain and strong winds (Appendix 1) which made it difficult to reach the shag nesting location. In addition to the weather being difficult, the birds were anxious and would fly out to sea at the slightest indication of human activity. There were also issues with tagged birds picking at the loggers until they fell off and cases where the tape used to fasten the loggers would loosen so they fell off, decreasing the number of logger units with data. What made it increasingly difficult to get enough shags as bio-drones was the sheer lack of birds within the seabird reserve. The low number of loggers may mean the data from the bio-drones shows an incomplete picture of shag foraging behavior at Runde, and that important foraging areas or other interesting trends went undetected during the study period.

4.2. Evaluation of UAV-based imaging of OOI in water column

There were some benefits to using the UAV during the surveys at Runde. It gave a larger area overview, and was able to identify OOI in the water column and shag behavior on land. Through this study it was found that the image quality from the UAV was affected by the light field (especially specular reflection) and IOP causing changes in the color and shape of the OOI. It was also found that contrast and distance between sensor and object were particularly important aspects of image quality.

4.2.1. UAV use at Runde for OOI above sea surface

While flying surveys, the UAV identified shags in flight, resting on islets, as well as common guillemots and puffins on the ocean surface. While maintaining an appropriate distance so as to not scare the seabirds, the UAV was able to count the number of individuals, and although this was an interesting observation, it did not indicate anything as to the health of the shag population nor their foraging behavior. Rather than using the UAV to map shag behavior in the conditions at Runde (small population with hidden nests), the technology seems more appropriate to use in open habitats above the sea surface (Jones, Pearlstine & Percival 2006). For environmental management, one must identify OOI, map OOI, and monitor OOI, and while previous studies have established UAVs as well suited for ecological monitoring on land (Rodríguez et al. 2012; Chabot & Bird 2015; Hodgson et al. 2017; Weimerskirch, Prudor & Schull 2018), the technology seems limited when searching for activities beneath the surface.

The results from the field work do imply that the shag is not a good study organism when using an aerial drone alone to map foraging or nesting behavior. The color of the shags' feathers is a drawback to using them as a study organism. The study at TBS found that the black Secchi disk as an imitation of a diving shag (Table 3.8) was the most difficult to identify in the water column as it could not be distinguished from the dark water masses. Not only would the birds be difficult to distinguish from the water masses once they submerge themselves, the diet samples from Runde illustrated that 76.22% of the shag's diet were foraged from the kelp forests, which structure would further obscure the birds from the UAV camera. Had the shags been foraging mainly in sandy substrates, the figurative rate of success could be higher, as the black feathers would contrast the light color of sand. However, it would still be difficult to record such an event with an aerial drone due to the complications of timing.

4.2.2. Change of image color as a function of depth

Data from the field study at Runde and the IOP Secchi disk experiment at TBS elucidate some of the imaging capabilities of a UAV as an instrument carrying platform and exemplify the increasing effect of IOP on color as a function of depth. At TBS images became more yellow because of high cDOM levels influencing image color (Table 3.9; Volent et al. 2011). In contrast, the colors of OOI at Runde became more blue as depth increased, due to the attenuation of red

light by water and low IOP (Fig. 3.7-Fig. 3.9). Because of this, the UAV was able to identify OOI to greater depths in the surveys near Runde than TBS.

In June, when the study at Runde was carried out, the Norwegian spring bloom of phytoplankton has ended causing low Chl-a concentration in the water masses and a low level of green coloration of OOI in the water column (Sakshaug 1997). The IOP concentrations were also low due to a large amount of moon and comb jellies having filtered the water for phyto- and zooplankton (Fossum et al. 2019). The case I (Fig. 1.2) water masses under these conditions made it possible for the UAV to map substrate types such as sand and kelp at both survey sites through the bottom effect (Fig. 1.4; Volent, Johnsen & Sigernes 2007). Identifying OOI with the UAV was successful at Runde since the low impact of IOP on color meant color could be used as an identifying characteristic of the OOI to a greater depth than in the Trondheimsfjord. Despite the low optical complexity however, there was still a darkening and homogenizing of colors in the OOI as depth increased, which made it more difficult to identify kelp forests below 3-5m depth (Fig. 3.7 and Fig. 3.9). In addition to IOP decreasing visibility, the attenuation of red light by water molecules caused the kelp growths (which were red-brown from 0 - 3m depth) to become dark blue at lower depths (Sakshaug, Johnsen & Volent 2009). This effect made it distinguishing kelp from other substrates like rocky or bedrock in the field more complicated, since the red color of kelp was no longer an identifiable characteristic.

At TBS the waters were much more turbid than at Runde, so that the UAV had difficulty determining the location of the Secchi disk already at 3m depth. The Secchi disk study took place after the wettest month of 2018 (Norwegian Meteorological Institute 2019). The large amount of precipitation and corresponding high river run-off caused there to be more cDOM in the water masses, making the optical conditions at TBS more complex (Table 3.2). This lead to color change and darkening of the OOI because of less upwelling light reaching the UAV sensor (Fig. 1.3 and Table 3.9). The IOP also caused homogenization of the colors so they all appear green, making it harder to distinguish the different Secchi disks and substrate types they mimic from each other (Table 3.3). Even though the optical conditions were very different between Runde and the Trondheimsfjord, the overall effect on image quality was similar. The color change, darkening, and homogenization caused by the IOP of water have a large impact on visibility and the UAVs ability to detect OOI in the water column. The degree to which IOP influence the

amount of information in remote sensing will vary strongly with season and cause a high variability to the success of the platform in spotting OOI. Although color change and darkening may not inhibit identification immediately at or beneath the water surface, researchers using this technology must be aware of the devaluation of color as a defining characteristic of the OOI when depth increases.

4.2.3. Contrast improving identification

The negative effects of color change on visibility were mitigated by the OOI having contrasting colors (Sakshaug, Johnsen & Sigernes 2009). This characteristic was seen in the Secchi disks, as the black & white and kelp & sand were the easiest to identify, while for the images of the black Secchi disk, often the contrast between the black disk and the white ROV were what allow the OOI to be identified (Appendix 3). A similar effect was found during surveys in the field, where the data from UAV-based imaging over Remøya indicated that the contrast between the sand and kelp forest allowed the two OOI to be distinguished. Contrast also became important for the UAV's ability to track the ROV during its transects. The visibility of the ROV was in part because the sea floor was mainly covered by kelp forests, contrasting the drone's white body (Fig. 2.4). Had the substrate been mostly sandy, most likely the visibility of the ROV would have been reduced due to the lack of contrast between it and the substrate beneath. Although it is possible to map the sea floor if the water is sufficiently clear and shallow, the contrast between a dark and light substrate does provide more certainty when using the UAV alone (without an ROV to confirm). It was noted that using a multi- or hyperspectral imaging sensor instead of an RGB sensor may have improved the UAV's ability to map substrate types by their color (Volent, Johnsen & Sigernes 2007), as these sensors would be less impacted by the attenuation of light changing OOI color.

4.2.4. Influence of light on image quality

The weather conditions were quite different between Runde and at TBS causing dissimilar light environments, though both impacted image quality. During the field surveys, glare from the diffuse light from the cloud cover had a large effect on the UAV's ability to spot OOI through the water column. This was particularly apparent during the Remøya survey, where the ROV could not be found due to the glare though it was only at ca. 1.5 m depth (Fig. 3.6). The issue was

remedied by changing the UAV camera angle in relation to the water surface to not be prependicular at 90°. Even though changing the position of the drone allowed the ROV to be found, it also changed the orientation of the image. When creating a photomosaic (merging pictures to create a large cover area), the change in camera orientation would transform the perspective and the photomosaic would be incoherent. Moreover, when using a UAV to detect animal behavior in the water column (species count, cetaceans surfacing, birds diving), the time it takes to re-orient the camera to reduce glare could mean the OOI is no longer within the frame.

At TBS on the other hand, the lack of cloud cover (0%; Norwegian Meteorological Institute 2019) and direct sunlight created a light environment where solar glints easily formed in images of OOI at the sea surface. When analyzing the UAV images of Secchi disks to find the RGB color value, the solar glints reduced the amount of information in the image thereby decreasing its quality. Hodgson, Kelly & Peel (2013) found that solar glints can cause as much as 50% of the image to be void of information. When using a UAV to count individual organisms or observe animal behaviors below the sea surface, the loss of information due to a poor light environment, both glints and glare, can significantly impact the efficacy of the technology and reduce the success of a mapping study.

To reduce the effects of specular reflection as both glare and solar glints, it was suggested that a polarizing filter (PF) should be tested on the UAV camera sensor. Although the PF will reduce specular reflection, its success is highly dependent on the angle of the sensor both to the sun and the sea surface. The study by Hodgson, Kelly & Peel (2013) found that using a PF was most beneficial when both the sun elevation angle and the camera's angle are 37 degrees from the surface of the water. However, when using a PF to conduct vertical remote sensing (sensor perpendicular to the sea surface) the filter had little to no effect on specular reflection, and it even decreases the exposure so that less light is received by the camera. It therefore seems a PF would not improve image quality under a survey of the type performed in this study, since large parts of the surveys were conducted with the sensor perpendicular to the ocean surface. The fact that a PF reduces exposure, making images darker also alludes to it being a poor choice, as OOI are already darkened as their depth increases.

Another way in which light impacted UAV image quality was through distortion by wave action on the sea surface (Fig. 4.1). Wave action also caused reflection on the sea surface to appear similar to a distorted Secchi disk, especially when looking for a Secchi in the lower range (3-5m) of depths (Fig. 4.2). The distorted Secchi disk is more likely to be confused with specular reflection because the shape of Secchi is not determinable from the image, influencing the interpretation of the images of an object of interest. The result of the distortion is that OOI no longer appear as they would above the surface, and the shape may no longer be a distinguishing characteristic when looking through water with the UAV.

Figure 4.1: Wave action modifying the shape of an OOI. The UAV image from 5m height of the kelp & sand colored Secchi disk at 1m depth showing how wave action changes the Secchi disk shape so that it is no longer quadratic. The movement at the sea surface may cause misinterpretation of OOI in the water column. Spatial resolution 259x263 pixels.

Figure 4.2: UAV image of either distorted Secchi disk or specular reflection, showing effect of light on image quality. The IOP cause the Secchi disk to appear dark, while the wave action distorts the image. The wave action also causes specular reflection, so that it is difficult to determine from this image whether the Secchi disk is the or not. The drone is at 10m elevation, and the kelp & sand Secchi at 5m depth. The poor spatial resolution of the image at this elevation makes it more difficult to identify the OOI. Spatial resolution 123x95 pixels

4.2.5. Spatial resolution as a function of distance

Even though the RGB sensor on the UAV provided a high resolution at 4K for images and video, there was a significant decrease in spatial resolution when distance to the OOI increased (Fig. 3.10). For accurate identification of OOI using the an RGB sensor, tracking and mapping studies will have to consider the sensor distance to the OOI, since zooming in on the image after the observation may not provide sufficient data because of the decrease in spatial resolution (Fig. 4.3). For example, when observing the puffins and common guillemots seen near Kaldekloven (Fig. 3.5) the UAV could not get closer than 15m before the birds dove beneath the surface. This made spatial resolution an important factor in image quality, since counting the individual birds from the images would be more difficult and less accurate if the image were too pixelated. Spatial resolution is particularly important for observing details in this example, since both puffins and common guillemots have black and white bodies, but can be differentiated by their beak color. For this reason, future applications of UAV technology have to be aware of the capacity of the camera sensor as well as the limitations of distance to the OOI and spatial resolution of UAV-based imaging for fine-scale data collection.
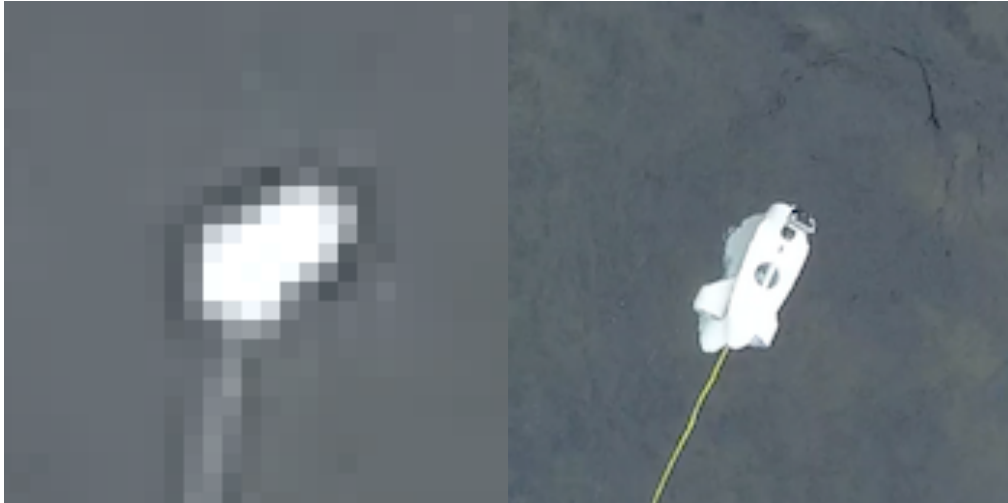
Figure 4.3: Decrease in spatial resolution with increased distance between the sensor and the OOI. When zooming in on the ROV in a UAV image taken from 60m elevation (Fig. 3.9), the level of detail in the ROV is very low, and the image is highly pixelated. In contrast, the zoom from 10m UAV elevation (Fig. 3.8) provides much more detail, since the spatial resolution of the image is higher. Spatial resolution, left image: 157x158 pixels; right image: 175x174 pixels.

4.2.6. Weather impacting UAV usage

The aerial drone model used in this study was not waterproof and could not fly in the rain, limiting deployment opportunities while in the field particularly in a wet climate like that at Runde (Norwegian Meteorological Institute 2019). The two surveys at Remøya and Kaldekloven were therefore completed on the same day, so that the AOP observed in the field are similar for both. If using UAVs in a wet environment, it would be an appropriate improvement to the study to use a different drone model since using a waterproof model would make the UAV less limited by rain, and it would be less risky to fly closer to the ocean surface.

The strong winds at the time of the field work (Appendix 1) made it difficult to fly the drone as desired as it was constantly blown off course. This also affected the video footage from the surveys, as much of the video was of the drone backing up or renegotiating its trajectory. Having to fly against the wind or double back on a flight path also drained the drone's batteries much quicker than less windy conditions would have. Under ideal conditions (no wind) the batteries of the UAV model used are expected to last maximum 30 minutes, but already at 30% battery charge the UAV will sound a "low battery" alarm and attempt to automatically land. Because of this feature, the 30 minute maximum was effectively 20 minutes as the drone was deployed from a boat and not on land and had to be manually maneuvered for landing. On account of the strong

winds during the field surveys (Appendix 1), the 20 minute time frame was reduced further to 10-15 minutes before the low battery alarm began. Not only did this reduce the amount of information obtained from the aerial drone since it could only fly for a short amount of time before having to change batteries, it also led to most of the survey time being spent taking off, landing, switching batteries and reorienting the drone according to the ROV position. It seems that using a different model may have mitigated the impact of weather on the UAVs flight capacity, as a heavier UAV would be more resistant to wind, and could carry longer-lived batteries.

4.3. Assessment of using three drones to identify important foraging habitats

In addition to studying the individual performance of the bio-drone, UAV, and ROV, this study aimed to evaluate the possibilities when combining data from the three instrument carrying mobile platforms. The three drones each contributed different perspectives on shag foraging behavior to create a comprehensive map of where and what the shags were targeting, but while the bio-drones and ROV provide in-depth insight into these aspects of shag behavior, the UAV contribution is limited because of the influences of AOP and weather on image quality.

The bio-drones were an important first step to guide the other two drones to where important foraging areas may be. Without the bio-drones being deployed first, the other two drones would have been driving blind and the information from the aerial and underwater drone would have been arbitrary in the mapping of important foraging habitats. For example, if an area had been chosen at random for a transect with the ROV and UAV, they may have found substrate types associated with shag dietary preferences as well as fish of appropriate size in this random location. Yet it may not be where the shags are foraging, and therefore unimportant for management or conservation. Although this study highlights advantages of using this three-part approach in mapping and monitoring of an indicator species, it should be mentioned that for decision making around important marine areas, studies must be done over the course of several breeding seasons to assure that any patterns observed are in fact important to the observed species and by extension the ecosystem.

Because it was submerged and gathered *in situ* data on the biodiversity and abundance in the transect area the information from the ROV was a valuable tool in terms of ecological insight and

extending the map of shag ecology. The ROV was found to be effective at identifying fish, in particular fish larger than 100mm in length (Strømsholm 2018). It should be pointed out that the success of the platform is in part due to the low IOP concentrations at the time of the study which allowed clear images of OOI beneath the surface (Zielinksi 2013; Fossum et al. 2019). The ROV was also used to explore an area where the shags were not diving to identify differences between areas with diving activity (Remøya) and without (Kaldekloven). ROV footage from Kaldekloven showed species like saithe and wrasse, which were found in the shag diet, yet the abundance of fish was low (Strømsholm 2018). Also, most of the observations were of fish estimated to be larger than 10cm, which is above the size range found through the back-calculation of fish size from the otoliths (Appendix 4). This information from the ROV can be used in management efforts, since the characteristics (kelp trawling, fishing activity, pollution, etc.) of important and unimportant areas can be compared to elucidate why there is a difference.

When using the UAV and ROV simultaneously in the survey areas, the UAV could be used to guide the ROV through its transect. Although it was not initially seen as a potential use for the UAV, this interaction between the ROV and the aerial drone was found to have potential in bettering the methodology since it improved the navigation of the underwater drone. Because the pilot was unable to see the submerged ROV during a transect, there were some challenges with navigating the underwater drone (see Strømsholm 2018). A bird's-eye view of the transect from the UAV gave the ROV pilot an overview of the ROV's orientation and direction so that the transects could be followed (Fig. 4.4). It also showed when the umbilical cord of the ROV got tangled, which happened when the ROV turned or when currents pulled at the umbilical. It should be noted that this, as other uses of the UAV, depend on the AOP during the survey, since high turbidity due to high IOP concentrations and glare or solar glints may prevent the ROV from being seen by the UAV (Fig. 3.6). Combining the UAV and ROV could hold great potential for applications in other fields as well. For instance, search and rescue missions in water could benefit from having one eye beneath the surface and another above to cover as much territory as possible. Also, marine archeology could use the combination of drones to search for OOI on the ocean floor, as is already done on land by hyperspectral imaging sensors on satellites (Kucukkaya 2004).

Figure 4.4: UAV tracking ROV to help it navigate as it moves through a transect above the kelp forests at Remøya. In the middle of the image is a pole indicating a subsea islet the ROV is trying to avoid. The ROV and its umbilical cord are both clearly visible despite the glare at the sea surface so the UAV could follow its movements. To avoid a collision, the ROV pilot used the live footage from the aerial drone to navigate this portion of the transect.

Using shags as indicator species by studying their diet samples has been argued as an effective indicator for overall ecosystem health (Frederiksen, Mavor & Wanless 2007; Lorentsen, Anker-Nilssen & Erikstad 2018). Yet when making decisions for management and conservation, it may seem insufficient to only look at one species within an entire ecosystem. Using the combination of bio- aerial- and underwater-drones as in this study created an integrated perspective of important shag foraging areas, but also the substrate types, local biodiversity, species abundance, and animal behaviors in the areas of interest. When using the shag as an indicator of ecosystem health, the expanded insight provided by the ROV with the help of the UAV could improve the accuracy of a study of ecosystem health, and potentially improve management efforts by providing more information for decision-making.

4.4. Future Prospects

While conducting the aerial surveys and processing the data, it became apparent that a standard for flying transects and a set of criteria for evaluating image quality would have improved the study. The European committee for standardization (CEN) approved in 2012 a standard (NS-EN

16260:2012) for visual seabed surveys using ROVs for collection environmental data. The standard outlines requirements for sensor position, calibration, transect speed and distance from seafloor, as well as a method for footage analysis post data collection. As per the deadline of this thesis (July 5th 2019), no such standard for UAV surveying of neither land nor sea has been implemented. The Single European Sky ATM Research Joint Undertaking (SESAR) released a report in 2016 outlining the need for a safety standard for a growing drone industry (SESAR 2016), yet there was no mention of a standardized method for UAV data collection and analysis although the uses of drones within mapping and monitoring are growing in relevance. Nilssen et al. (2015) suggests a generic approach to aid in selecting mobile platform types, sensors, and methodology for environmental mapping, but again there is a lack of a standardized approach to data analysis of UAV footage. The American Society for Photogrammetry and Remote Sensing (ASPRS) published an accuracy standard for large scale maps created by remote sensing. Similar to the push broom technique (Volent, Johnsen & Sigernes 2007), the standard contains guidelines for testing accuracy, horizontal and vertical controls, and using spatial accuracy as a gauge for mapping precision (ASPRS 1990). Although both SESAR and ASPRS are addressing important aspects of remote sensing and UAV use, neither present a code of conduct for data collection or analysis. As small UAVs are becoming increasingly popular in ecological surveys, the lack of a standard like the NS-EN 16260:2012 for aerial remote sensing seems necessary. Having such a standard would improve the quality of studies using UAVs, as surveys and image analysis would follow a quality control. It would also reduce human bias and fallibility, as even researchers are prone to make errors (Soros 2014). Furthermore, a standard would ensure comparability between studies, and would make it easier for future studies to build on pre-existing knowledge.

Since ROV and UAV were good to use together, it would have been an interesting augmentation of the study to have the two platforms follow preprogrammed transects in the survey area. Such transects would be limited by the aerial drone's battery life, which is short compared to the ROV's. It would also be restricted by the UAV's ability to see through the water column. A method where the two mobile platforms follow the same transect would create a data set more statistically sound than the exploratory tests done in this study. It would also be an easier methodology to develop a standard for data collection and analysis, as the ROV and UAV would follow pre-determined trajectories.

A final suggestion to widen the scope of this study would be to deploy the UAV with a hyperspectral imager in addition to, or rather than an RGB sensor. Though AOP and spatial resolution would still be important factors determining image quality, a sensor with a larger spectral range will be able to separate substrates of similar color despite the darkening effects of water. For example, the different color signatures from kelp and stone that are not registered by an RGB sensor could be distinguished with hyperspectral imaging (Volent et al. 2007). This would also allow accurate substrate mapping to further depths than with an RGB sensor alone.

5. Conclusion

Though a pilot study, the present study highlights advantages and challenges of using instrument carrying mobile platforms in ecological studies with the shag as a model organism. Over the course of this work, it has been found that:

- Using the combination of bio- aerial- and underwater-drones in this study provided comprehensive insight into important shag foraging areas, including the substrate types and depths, local biodiversity, species abundance, and animal behaviors in the areas of interest.
- The three part approach used in this study indicates that the bio-drones should be deployed first to ensure that the information from the UAV and ROV in the survey areas is relevant to the foraging behavior of the study organism.
- Bio-drones provide important data for determination of important flight routes and foraging areas for shags and these areas may by extension be important for the ecosystem. However, this type of tracking study has to be done over longer periods of time and over multiple breeding seasons to correctly identify important marine areas for monitoring purposes.
- The ROV is a good supplement to the information provided by the bio-drones as it can observe the foraging area (bottom substrate types and distribution, species diversity) *in situ.*
- The UAV identified shags in flight, resting on islets, as well as common guillemots and puffins on the ocean surface, but the technology was limited in terms of observing foraging behavior.
- Based on seabird observations made at Runde with the UAV, a sensor with the highest quality (at least 4K) is needed to ensure sufficient image spatial resolution for species identification and counting of individual organisms in the UAV images. During seabird survey, the UAV camera sensor should be no more than 50m away from the OOI to get an

overview, and for detailed seabird observations (i.e. using characteristics such as beak color) the UAV sensor should be no more than 15m away from the OOI.

- The low IOP concentrations at Runde enabled the UAV to identify OOI to a greater depth than at in the Trondheimsfjord site with relatively higher IOP concentrations. However, as OOI depth increased, color composition as became an unreliable characteristic for OOI identification at both locations. This was due to less upwelling light being received by the UAV camera causing darkening of images, IOP changing the color of OOI, and the combination of the two leading to homogenization of color making it hard to identify OOI.

- Contrast in the OOI mitigated the effect of color homogenization, so that they could be recognized to at greater depths than more monochromic UAV images of OOI.

- Spatial resolution of UAV images decreased with elevation, lowering image quality and making it more difficult to use identify OOI, such as beak color to distinguish between puffins and common guillemots at the sea surface.

- The ability of the UAV to adjust for variable weather conditions and the many environmental factors influencing image quality limits the information on OOI when used in marine field studies. Even so, there is potential for this technology, and different UAV models (larger and more weather resistant) with different sensors (multi- or hyperspectral imagers) should be tested to see if these alterations may mitigate the effects of AOP on image quality.

- Although providing limited value in terms of information on foraging behavior, the UAV was valuable in navigating the ROV through its transects, and the combination of technologies may hold value for application in other activities. However, a standard method such as the NS-EN 16260:2012 should be developed for data collection and analysis by the UAV to improve survey quality and enable comparability between future studies.

- The methodology is transferable to other study organisms as indicator species, and can potentially improve nature management efforts by providing more information for decision-making in important marine areas.

References

References follow the template for the Harvard referencing style.

Andersen K, Chapman, A, Hareide, NR, Folkestad, AO, Sparrevik, E & Langhamer O 2009, 'Environmental monitoring at the Maren wave power test site off the island of Runde, western Norway: planning and design', in *Proceedings of the 8th European Eave and Tidal Energy Conference*, Uppsala, Sweden, 2009, pp. 1029-1038.

Azis, FA, Aras, MSM, Rashid, MZA & Othman, MN 2012, 'Problem identification for underwater remotely operated vehicle (ROV): A case study', *Procedia Engineering,* vol. 41, pp. 554-560, DOI: 10.1016/j.proeng.2012.07.211.

Barrett, R, Lorentsen, S & Anker-Nilssen, T 2006, 'The status of breeding seabirds in mainland Norway', *Atlantic Seabirds,* vol. 8, no. 3, pp. 97-126.

Barrett, RT & Furness, RW 1990, 'The prey and diving depths of seabirds on Hornoy, north Norway, after a decrease in the Barents Sea capelin stocks', *Scandinavian Journal of Ornithology,* vol. 21 no. 3, pp. 176-186, DOI: 10.2307/3676777.

Borelle, SB & Fletcher, AT 2017, 'Will drones reduce investigator disturbance to surface nesting birds', *Marine Ornithology,* vol. 45, no. 1, pp. 89-94.

Bustnes, JO, Anker-Nilssen, T, Erikstad, KE, Lorentsen, S & Systad, GH 2013, 'Changes in the Norwegian breeding population of European shag correlate with forage fish and climate', *Marine Ecology Progress Series,* vol. 489, pp. 235-244, DOI: 10.3354/meps10440.

Campbell, J & Wynne, RH 2011, 'History and Scope of Remote Sensing' in *Introduction to Remote Sensing*. The Guilford Press, New York, pp. 3-22.

Cairns, DK 1988, 'Seabirds as indicators of marine food supplies', *Biological Oceanography*, vol. 5, no. 4, pp. 261-271, DOI: 10.1080/01965581.1987.10749517.

Ceballos, G, Ehrlich, PR, Barnosky, AD, García, A, Pringle, RM, & Palmer, TM 2015, 'Accelerated modern human-induced species losses: Entering the sixth mass extinction', *Environmental Sciences,* DOI: 10.1126/sciadv.1400253.

Chabot, D & Bird, DM 2015, 'Wildlife research and management methods in the 21st century: Where do unmanned aircraft fit in?', *Journal of Unmanned Vehicle Systems,* vol. 3, pp. 137-155, DOI: 10.1139/juvs-2015-0021.

Christensen-Dalsgaard, S, Mattison, J, Bekkby, T, Gundersen, H, May, R, Rinde, E, & Lorentsen, S-H 2017, 'Habitat selection of foraging chick-rearing European shags in contrasting marine environments' *Marine Biology,* vol. 164, no. 196, DOI: 10.1007/s00227-017-3227-5.

Crain CM, Kroeker, K, & Halpern BS 2008, 'Interactive and cumulative effects of multiple human stressors in marine systems', *Ecology Letters* vol. 11, pp. 1304-1315, DOI: 10.1111/j.1461-0248.2008.01253.x.

Croxall, JP, Butchart, SHM, Lascelles, B, Stattersfield, AJ, Sullivan, B, Symes, A & Taylor, P 2012, 'Seabird conservation status, threats and priority actions: a global assessment', *Bird Conservation International* vol. 22, pp. 1-34, DOI: 10.1017/S0959270912000020.

Ermayanti, Z, Apriliani, E, Nurhadi, H & Herlambang, T 2015, 'Estimate and control position autonomous underwater vehicle based on determined trajectory using fuzzy kalman filter method' in *International Conference on Advanced Mechatronics, Intelligent Manufacture, and Industrial Automation 2015* (ICAMIMIA 2015), Surbaya, Indonesia, Oct. 15-17, 2015.

Falkowski, PG & Raven, J 2007, *Aquatic Photosynthesis,* 2nd edition. New Jersey: Princeton University Press.

Fey, DP & Linkowski, TB 2006, 'Predicting juvenile Baltic cod (*Gadus morhua*) age from body and otolith size measurements', *ICES Journal of Marine Science* vol. 63, pp. 1045-1052, DOI: 10.1016/j.icesjms.2006.03.019.

Fortin, M, Bost, CA, Maes, P, & Barbraud, C 2013, 'The demography and ecology of the European shag *Phalacrocorax aristotelis* in Mor Braz, France', *Aquat. Living Resour.* vol. 26, no. 2, pp. 179-185, DOI: 10.1051/alr/2012041.

Fossum, TO, Fragoso, GM, Davies, EJ, Ullgren, JE, Mendes, R, Johnsen, G, Ellingsen, I, Eidsvik, J, Ludvigsen, M, & Rajan, K 2019, 'Toward adaptive robotic sampling of phytoplankton in the coastal ocean. *Science Robotics,* vol. 4, DOI: 10.1126/scirobotics.aav3041.

Frederiksen, M, Mavor, RA & Wanless, S 2007, 'Seabirds as environmental indicators: the advantages of combining data sets', *Marine Ecology Progress Series,* vol. 352, pp. 205-211, DOI: 10.3354/meps07071.

Garcia, R, Nicosevici, T, & Cufi, X 2002, 'On the way to solve lighting problems in underwater imaging', *Proceedings of the IEEE Oceans Conference Record*, Biloxi, MI, U.S.A., pp. 1018–1024.

Grémillet, D & Boulinier, T 2009, 'Spatial ecology and conservation of seabirds facing global climate change: a review', *Marine Ecology Progress Series*, vol. 391, pp. 121-137. DOI: 10.3354/meps08212.

Härkönen, T 1986, *Guide to the otoliths of the bony fishes of the Northeast Atlantic*, Danbiu ApS. Biological consultants, Hellerup, Denmark.

Hillersøy, G & Lorentsen, S-H 2012, 'Annual variation in the diet of breeding european shag (*Phalacrocorax aristotelis*) in Central Norway', *Waterbirds*, vol. 35, no. 3, pp. 420–429.

Hodgson, A, Kelly, N, & Peel, D 2013, 'Unmanned aerial vehicles (UAVs) for surveying marine fauna: A dugong case study', *PLoS ONE,* vol. 8, no. 11, DOI: 10.1371/journal.pone.0079556.

Hodgson, JC, Mott, R, Baylis, SM, Pham, TT, Wotherspoon, S, Kilpatrick, AD, Segaran, RR, Reid, I, Terauds, A, & Koh, LP 2017, 'Drones count wildlife more accurately and precisely than humans', *Methods in Ecology and Evolution,* vol. 1, no. 8, DOI: 10.1111/2041-210X.12974.

Howell, RJ, Burthe, SJ, Green, JA, Harris, MP, Newell, MA, Butler, A, Wanless, S, & Daunt, F 2018, 'Pronounced long-term trends in year-round diet composition of the European shag *Phalacrocorax aristotelis*', *Marine Biology,* pp. 165-188, DOI:10.1007/s00227-018-3433-9.

Hyrenbach, KD, Forney, KA, & Dayton, PK 2000, 'Marine Protected Areas and Ocean Basin Management', *Aquatic Conservation: Marine and Freshwater Ecosystems*, vol. 10. pp. 427-458.

IOCCG 2000, 'Remote Sensing of Ocean Color in Coastal, and Other Optically-Complex Waters' in Sathyendranath, S (ed), *Reports of the International Ocean-Color Coordinating Group, No. 3.* IOCCG, Dartmouth, Canada.

IUCN 2019, *The IUCN Red List of Threatened Species. Version 2019-1*. <http://www.iucnredlist.org<, viewed 21 March 2019.

Jobling, M & Breiby, A 1986, 'The use and abuse of fish otoliths in studies of feeding habits of marine piscivores', *Sarsia* vol. 71, pp. 265–274.

Johnsen, G, Volent, Z, Sakshaug, E, Sigernes, F, & Petterson, LH 2009, 'Remote sensing in the Barents Sea' in E Sakshaug, G Johnsen & K Kovacs (eds), *Ecosystem Barents Sea*, 1st ed. Trondheim, Tapir Academic Press, pp. 139-165.

Johnsen, G, Volent, Z, Dierssen, H, Pettersen, R, Ardelan, M, Søreide, F, & Fearns, P 2013, 'Underwater hyperspectral imagery to create biogeochemical maps of seafloor properties' in J Watson & O Zielinski (eds), *Subsea Optics and Imaging*, Woodhead publishing, pp. 508-535.

Jones, GP, Pearlstine, LG, & Percival, FH 2006, 'An assessment of small unmanned aerial vehicles for wildlife research', *Wildlife Society Bulletin*, vol. 34, no. 3, pp. 750-758, DOI: 10.2193/0091-7648.

Kucukkaya, AG 2004, 'Photogrammetry and remote sensing in archelogy', *Journal of Quantitative Spectroscopy and Radiative transfer*, Vol. 88, no. 1-3, pp. 83-88, DOI: 10.1016/j.jqrst.2003.12.030.

Lewison, R, Oro, D, Godley, BJ, Underhill, L, Bearhop, S, Wilson, RP, Ainley, D, Arcos, JM, Boersma, PD, Borboroglu, PG, Boulinier, T, Frederiksen, M, Genovart, M, Gonzáles-Solis, J, Green, JA, Grémillet, D, Hamer, KC, Hilton, GM, Hyrenbach, KD, Martínez-Abraín, A, Montevecchi, WA, Phillips, RA, Ryan, PG, Sagar, P, Sydeman, WJ, Wanless, S, Watanuki, Y, Weimerskirch, H & Yorio, P 2012, 'Research priorities for seabirds: improving conservation and management in the 21st century', *Endagered Species Research,* vol. 17, pp. 93-121, DOI: 10.3354/esr00419.

Lorentsen, SH, Anker-Nilssen, T, Erikstad, KE & Røv, N 2015, 'Forage fish abundance is a predictor of timing of breeding and hatching brood size in a coastal seabird', *Marine Ecology Progress Series,* vol. 519, pp. 209-220, DOI: 10.3354/meps11100.

Lorentsen, SH, Anker-Nilssen, T & Erikstad, KE 2018, 'Seabirds as guides for fisheries management: European shag *Phalacrocorax aristotelis* diet as indicator of saithe *Pollachius virens* recruitment', *Marine Ecology Progress Series*, vol. 586. pp. 193-201, DOI: 10.3354/meps12440.

Ludvigsen, M 2010, 'An ROV toolbox for optical and acoustical seabed investigations', Ph.D. thesis, Norwegian University of Science and Technology, Faculty of Engineering Science and Technology, Dept. of Marine Technology.

Ludvigsen, M, Johnsen, G, Sørensen, AJ, Lågstad, PA & Ødegård, Ø 2014, 'Scientific operations combining ROV and AUV in the Trondheim Fjord', *Marine Technology Society Journal*, vol. 48, no. 2, pp. 59-71, DOI: 10.1109/OCEANS-Bergen.2013.6608194.

Mallory, ML, Robinson, SA, Hebert, CE & Forbes, MR 2010, 'Seabirds as indicators of aquatic Ecosystem conditions: A case for gathering multiple proxies of seabird health', *Marine Pollution Bulletin*, vol. 60, pp. 7-12, DOI: 10.1016/j.marpolbul.2009.08.024.

Mobley CD 2010, 'The optical properties of water', chapter 43 in *Handbook of Optics,* 3rd edn*,* McGraw Hill Professional, New York, pp. N/A.

Naito, Y 2004, 'Bio-logging science and new tools for marine bio-science' *Proceedings of the International Symposium on SEASTAR2000 and Bio-logging Science,* The 5th SEASTAR2000 Workshop, pp. 72-75.

NBIC, 2019, *Toppskarv* Phalacrocorax aristotelis *(Linnaeus, 1761),* Norwegian Biodiversity Information Centre, viewed 25 Jun. 2019, <https://artsdatabanken.no/Taxon/Phalacrocorax%20aristotelis/3933>.

Nilssen, I, Ødegård, Ø, Sørensen, AJ, Johnsen, G, Moline, MA & Berge, J 2015, 'Integrated environmental mapping and monitoring, a methodological approach to optimize knowledge gathering and sampling strategy', *Marine Pollution Bulletin,* vol. 96. pp. 374-383, DOI: 10.1016/j.marpobul.2015.04.045.

Norwegian Meteorologisk Institute 2019, Meteorologisk Institutt, accessed 2 Apr. 2019, <http://sharki.oslo.dnmi.no/portal/page?_pageid=73,39035,73_39049&_dad=portal&_sch sch=PORTAL>.

Paleczny, M, Hammill, E, Karpouzi, V & Pauly, D 2015, 'Population trend of the world's monitored seabirds, 1950-2010' *PLoS ONE,* vol. 10, no. 6, DOI: 10.1371/journalpone.0129342.

Parsons, M, Mitchell, I, Butler, A, Ratcliffe, N, Frederiksen, M, Foster, S & Reid, JB 2008, 'Seabirds as indicators of the marine environment', *ICES Journal of Marine Science*, vol. 65, no. 8, pp. 1520-1526, DOI: 10.1093/icesjms/fsn155.

Preisendorfer, RW 1986, 'Secchi disk science: Visual optics of natural waters', *Limnology and Oceanography*, vol. 31, no. 5, pp. 909-926.

Rodríguez, A, Negro, JJ, Mulero, M, Rodríguez, C, Hernández-Pliego, J & Bustamante, J 2012, 'The eye in the sky: Combined use of unmanned aerial systems and GPS data loggers for ecological research and conservation of small birds', *PLoS ONE*, vol. 7, no. 12, DOI: 10.1371/journal.pone.0050336.

Sakshaug, E 1997, 'Biomass and productivity distributions and their variability in the Barents Sea', *ICES Journal of Marine Science*, vol. 54, pp. 341–350.

Sakshaug, E, Johnsen, G & Volent, Z 2009, 'Light' in E Sakshaug, G Johnsen & K Kovacs (eds) *Ecosystem Barents Sea*, 1st ed. Trondheim: Tapir Academic Press, pp. 117-138.

Schettini, R & Corchs, S 2009, 'Underwater image processing: state of the art of restoration and image enhancement methods', *EURASIP Journal on Advances in Signal Processing*, DOI: 10.1155/2010/46052.

SESAR 2016, *European drones outlook study: Unlocking the value for Europe,* Single European Sky ATM Research, EU, viewed 25 May 2019, <https://www.sesarju.eu/sites/default/files/documents/reports/European_Drones_Outlook_Stu St_2016.pdf>.

Soanes, LM, Arnould, JPY, Dodd, SG, Milligan, G & Green, JA 2014, 'Factors affecting the foraging behaviors of the European shag: implications for seabird tracking studies', *Marine Biology* vol. 161, pp. 1335-1348, DOI: 10.1007/s00227-014-2422-x.

Soros, G 2014, 'Fallibility, reflexivity, and the human uncertainty principle', *Journal of Economic Methodology*, vol. 20, no. 4, pp. 309-329, DOI: 10.1080/1350178X.2013.859415.

Söffker, M, Sloman, KA & Hall-Spencer, JM 2011, '*In situ* Observations of Fish Associated with Coral Reeds off Ireland' *Deep-Sea Research I*, vol. 58, pp. 818-825.

Strømsholm, J 2018, 'Eyes beaneth the surface: using a miniROV to reveal the habitat and dietary choices of the European shag'. s.l:s.n.

Swann, RL, Harris, MP, & Alton, DG 2008, 'The diet of European Shag Phalacrocorax aristotelis, Black-legged Kittiwake Rissa tridactyla and Common Guiellemot Uria aalge on Canna during the chick-rearing period 1981-2007', *Seabird,* vol. 21, pp. 44-54.

Valle, KC, Nymark, M, Aamot, I, Hancke, K, Winge, P, Andersen, K, Johnsen, G, Bremby, T & Bones, AM 2014, 'System response to equal doses of photosynthetically usable radiation of blue, green, and red light in the marine diatom *Phaeodactylum tricornutum*' *PLoS One,* vol. 9, no. 12, DOI: 10.1371/journal.pone.0114211.

Volent, Z, Johnsen, G, & Sigernes, F 2007, 'Kelp forest mapping by use of airborne hyperspectral imager' *Journal of Applied Remote Sensing,* vol. 1, DOI: 10.1117/1.2822611.

Volent, Z, Johnsen, G, Hovland, EK, Folkestad, A, Olsen, LM, Tangen, K & Sorensen, K 2011, 'Improved monitoring of phytoplankton bloom dynamics in a Norwegian fjord by integrating satellite data, pigment Analysis, and Ferrybox data with a coastal observation network', *Journal of Applied Remote Sensing,* vol. 5, no. 1, DOI: 10.1117/1.3658032.

Wakefield, ED, Phillips, RA & Matthiopoulos, J 2009, 'Quantifying habitat use and preferences of pelagic seabirds using individual movement data: a review' *Marine Ecology Progress Series*, vol. 391. pp. 165-182, DOI: 10.3354/meps08203.

Warwick-Evans, VC, Atkinson, PW, Robinson, LA & Green, JA 2016, 'Predictive modelling to identify near-shore, fine-scale seabird distributions during the breeding season', *PLoS ONE,* vol. 11, no. 3, DOI:10.1371/journal.pone.0150592.

Watanuki, Y, Daunt, F, Takahashi, A, Newell, M, Wanless, S, Sato, K & Miyazaki, N 2008, 'Microhabitat use and prey capture of a bottom-feeding top predator, the European shag, shown by camera loggers', *Marine Ecology Progress Series,* vol. 356, pp. 283-293, DOI: 10.3354/meps07266.

Weimerskirch, H, Prudor, A, & Schull, Q 2018, 'Flights of drones over sub-Antarctic seabirds show species- and status-specific behavioral and physiological responses' *Polar Biology*, vol. 41. pp. 259-266, DOI: 10.1007/s00300-017-2187-z.

Wilmers, CC, Nickel, B, Bryce, CM, Smith, JA, Wheat, RE & Yovovich, V 2015, 'The golden age of bio-logging: how animal-borne sensors are advancing the frontiers of ecology' *Ecology*, vol. 96, no. 7, pp. 1741-1753.

WoRMS 2019, World Register of Marine Species, viewed 28 Jan 2019, <http://www.marinespecies.org/>.

Zielinski, O 2013, 'Subsea optics: an introduction' in J Watson & O Zielinski eds, *Subsea Optics and Imaging*, 1st edition. Philadelphia: Woodhead Publishing Limited, pp. 3-33.
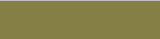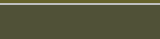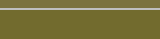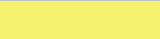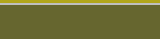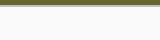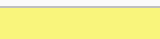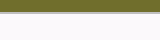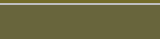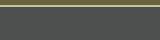
Appendix 1: Weather during field work

Table 0.1: Weather during Runde excursion, giving the average temperature, cloud cover and wind speed during study. The wind speed impacted the drones, since strong winds prevented the aerial drone from being flown safely, and created waves too big for safe use of the ROV. Partial cloud cover is 40-60% cloud coverage of the sky, mostly cloud covered is 70-80%, broken cloud cover 90%, while total cloud cover is 100%. Both the wind levels and cloud cover have been named according to the Norwegian Meteorological Institute (Meteorologisk institutt 2019).

Date	Average temp. (°C)	Wind	Precipitation (mm)	Cloud cover (None/Partial/Total)
14.06.17	7.1	Light breeze (2.0 m/s)	0.5	Partial
15.06.17	7.3	Gentle breeze (4.1 m/s)	1.6	Total
16.06.17	7.7	Gentle breeze (5.2 m/s)	2.6	Total
17.06.17	13.3	Strong breeze (10.9 m/s)	1.9	Total
18.06.17	11.9	Near gale (16.3 m/s)	7.6	Total
19.06.17	11.3	Near gale (15.4 m/s)	2.9	Total
20.06.17	9.4	Fresh breeze (10.4 m/s)	11.7	Total
21.06.17	10.0	Gentle breeze (4.9 m/s)	3.2	Total
22.06.17	11.8	Gentle breeze (3.8 m/s)	0.1	Total
23.06.17	12.2	Gentle breeze (3.6)	0	Total
24.06.17	12.2	Moderate breeze (7.3 m/s)	2.6	Total
25.06.17	12.1	Fresh breeze (7.6 m/s)	0.7	Partial
26.06.17	9.9	Fresh breeze (8.7 m/s)	3.0	Partial
27.06.17	10.1	Gentle breeze (5.2 m/s)	2.9	Partial

Appendix 2: RGB color values

Table 0.2: Overview of results from RGB image analysis with dynamic range of 8 bits. The average RGB color number (n=50) for each Secchi disk color at the various height and depth intervals is shown. The color resulting from those RGB color values is also shown. As the colors demonstrate, there is a clear rise in yellow hue as the Secchi depth increases. However, they also suggest that the aerial drone's ability to capture color intensity decreases with height, as the colors get less intense at same depth of Secchi disk but increased height of camera.

Disk color	Aerial drone height (m)	ROV depth (m)	Average Red	Average Green	Average Blue	Color
Black (of black and white disk)	5	0	87.9	72.3	95.16	
	5	1	132.56	127.04	69.32	
	5	2	102.38	97.94	43.84	
	5	3	80.3	80.94	54.64	
	10	0	97.82	84.72	95.72	
	10	1	122.52	114.06	61.9	
	10	2	113.72	107.26	46.08	
	10	3	84.38	83.28	50.9	
	30	0	91.36	85.56	101.98	
	30	1	124.62	115.42	52.26	
	30	2	115.1	106.44	40.88	
	30	3	77.3	78.18	49.86	
White (of black and white disk)	5	0	254.94	254.78	254.92	
	5	1	247.08	241.44	112.3	
	5	2	178.26	166.1	26.72	
	5	3	101.76	102.24	46.78	
	10	0	250.68	250.02	250.48	
	10	1	248.94	245.44	123.66	
	10	2	205.46	189.8	24.9	
	10	3	111.54	109.7	44.18	
	30	0	250.88	249.4	251.02	
	30	1	242.94	238.32	105.6	
	30	2	176.88	167.14	38	
	30	3	100.98	103.04	51.66	
Kelp (of kelp and sand disk)	5	0	179.58	121.86	81.9	
	5	1	158.08	134.9	69.46	
	5	2	116.02	108	42.3	
	5	3	103.6	101.04	60.08	
	5	5	76.64	78.58	77.96	
	10	0	204.42	148.26	104.8	
	10	1	163.3	135.02	50.7	

	10	2	142.48	127.76	62.52	
	10	3	113.18	110.38	59.3	
	10	5	70.08	76.94	57.62	
	30	0	210.74	173.3	159.24	
	30	1	138.92	125.52	57.28	
	30	2	140.84	134.52	41.06	
	30	3	93	92.94	49.18	
Sand (of kelp and sand disk)	5	0	251.6	251.12	250.96	
	5	1	253.04	248.64	122.08	
	5	2	188.82	175.12	28.28	
	5	3	137.06	133.9	49.36	
	5	5	84.7	87.94	80.34	
	10	0	254.32	254.12	253.9	
	10	1	252.32	249	130.4	
	10	2	225.06	208.78	54.86	
	10	3	151.24	149.54	49.34	
	10	5	76.02	80.72	70.96	
	30	0	252.76	251.52	251.32	
	30	1	250.92	246.62	133	
	30	2	203.7	201.42	49.64	
	30	3	117.34	120.32	46.16	
Black	5	0	82.12	69.74	92.54	
	5	1	78.6	74.76	67.76	
	5	2	88.7	85.56	49.84	
	5	3	70.46	70.7	52.76	
	10	0	83.62	70.3	90.92	
	10	1	73.44	69.92	67.78	
	10	2	102.28	97.6	57.2	
	10	3	87.28	84.64	44.96	
	10	5	55.94	61.24	57.36	
	30	0	77.6	62.88	79.38	
	30	1	81.84	77.42	70.12	
	30	2	78.06	76.3	68.08	
	30	3	63.86	65.92	59.54	

Appendix 3: Images of Secchi disks

Table 0.3: UAV images of black & white Secchi disk at several depths and altitudes to illustrate the IOP effect on image quality at different distances and depths. The Secchi disk was mounted on the ROV. The pictures are cropped to frame the Secchi disk. Because of the increase in height of the aerial drone, the spatial resolution of the images decreases with height. At 5m elevation, resolution is 382 x 343 pixels, at 10m elevation 131 x 132 pixels, and at 30m 34 x34 pixels. These images were then processed for the RGB analysis shown in table 3.2.. As neither the Secchi disk nor the ROV were visible at 5m depth and 30m height, the image was omitted.
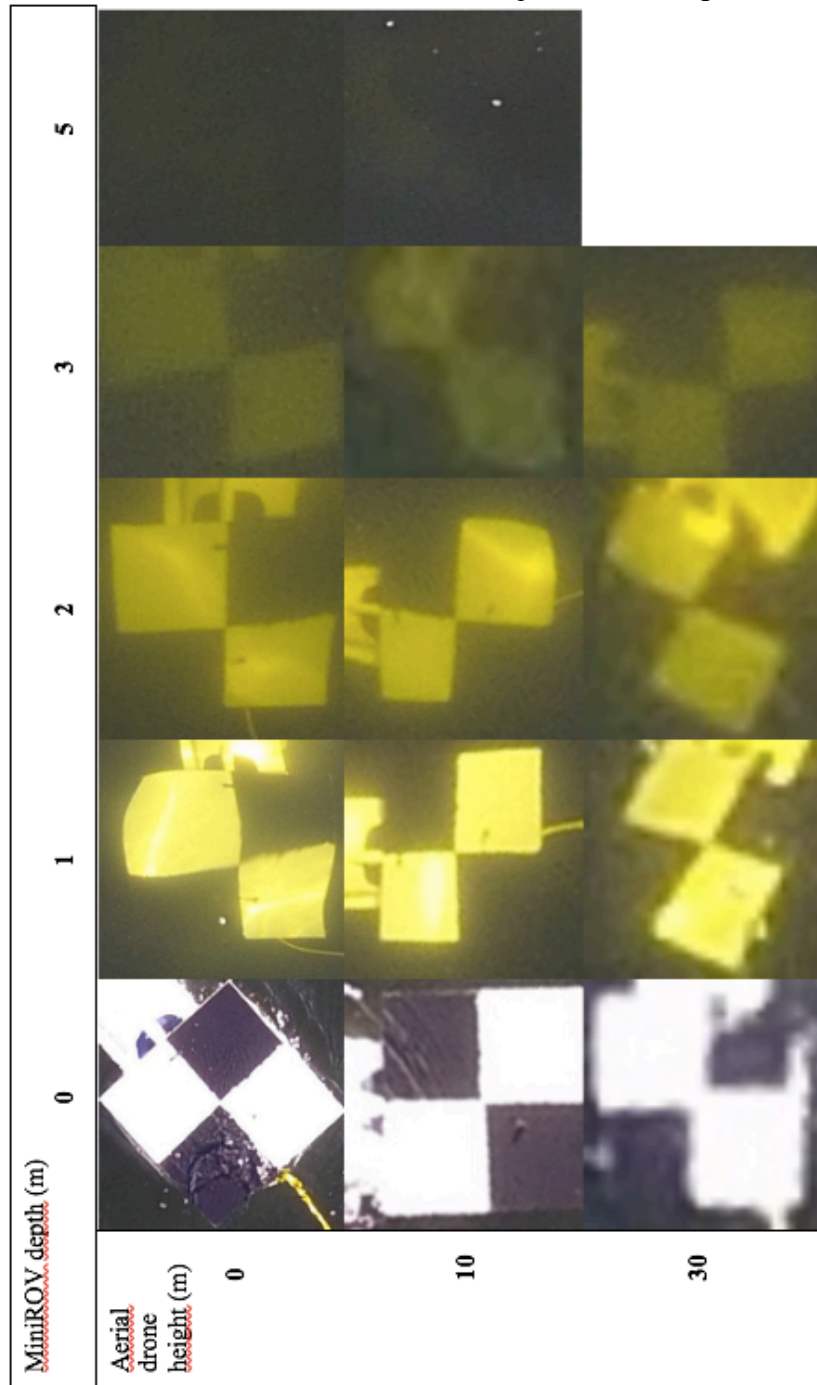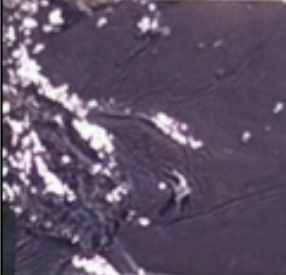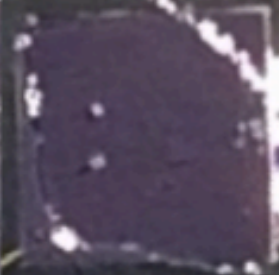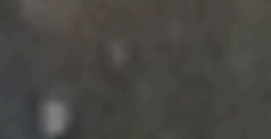
Table 0.4: Aerial drone images of Secchi at several depth and altitudes of the black Secchi disk mounted on the ROV. The pictures have been cropped to frame the Secchi disk. Because of the increase in height of the aerial drone, the spatial resolution of the images decreases with height. At 5m elevation, resolution is 382 x 343 pixels, at 10m elevation 131 x 132 pixels, and at 30m 34 x34 pixels. These images were then processed for the RGB analysis, shown in table 3.2. Images at 5m depth have been omitted as neither the Secchi disk nor ROV could be discerned from the images.

Appendix 4: Otolith length and back-calculation of fish length

Table 0.5: Length of otoliths from shag pellets. n=1690, plus 138 otoliths which were broken. The whole otoliths could then be used to back-calculate the length of the fish the shags were eating.

English name	Latin name	Otolith length (mm)				
		Min	Mean	Max	SD	n
Sand lance	Ammodytidae (Bonaparte, 1832)	1.2	1.79	2.2	0.11	129
Longspined bullhead	*Taurulus bulbalis* (Gratzianov, 1907)	1.1	2.0	2.9	0.43	75*
Cottidae indet.		1.7	1.7	1.7	0	1
Atlantic cod	*Gadus morhua* (Linneus, 1758)	3	6.66	1.7	0.31	6
Pollack	*Pollachius pollachius* (Linneus, 1758)	4.7	6.19	7.2	0.59	33
Poor cod	*Trisopterus minutus* (Linneus, 1758)	2.5	5.43	9.5	0.98	345*
Shore rockling	*Gaidropsarus mediterraneus* (Linneus, 1758)	2.2	2.58	3.2	0.3	8*
Saithe	*Pollachius virens* (Linneus, 1758)	3	4.67	10	2.08	70*
Tadpole fish	*Raniceps raninus* (Linneus, 1758)	4.3	4.45	4.6	0.15	2
Gadidae indet.		1.1	2.34	7.4	0.69	631*

Black goby	*Gobius niger* (Linneus, 1758)	3.7	3.7	3.7	0	2
Gobidae indet.	(Cuvier 1816)	0.5	0.86	1.5	0.3	17
Cuckoo wrasse	*Labrus mixtus* (Linneus, 1758)	4.2	4.25	4.3	0.05	4
Corkwing wrasse	*Symphodus melops* (Linneus, 1758)	1.9	2.22	2.8	0.28	13
Golsinny wrasse	*Ctenolabrus rupestris* (Linneus, 1758)	2.2	2.53	2.9	0.22	16
Labridae indet.	(G. Cuvier, 1816)	0.9	1.83	4.2	0.58	307*
Common ling	*Molva molva* (Linneus, 1758)	4.8	5.74	7.2	0.8	9
Rock gunnel	*Pholis gunnel* (Linneus, 1758)	0.8	1.67	1.7	0.31	6
Flatfish	(Linneus, 1758)	1.7	1.93	2.4	0.21	9
Viviparous eelpout	*Zoarces viviparus* (Linneus, 1758)	1.5	1.56	1.6	0.05	7

*Broken otoliths: Longspined bullhead 2, Labridae indet 26, Pollack 1, Saithe 17, Poor cod 12, Shore rockling 1, Atlantic cod 79.

Table 0.6: Fish length back-calculated from otoliths. The largest fish identified was a saithe 304.04mm long, the smallest a Gobiidae indet. of 11.93mm. Mean length for all fish found was 96.49mm.

English name	Latin name	Min	Mean	Max	SD	n
Sand lance	Ammodytidae (Bonaparte, 1832)	68.92	99.03	120.22	6.16	99
Longspined bullhead	*Taurulus bulbalis* (Gratzianov, 1907)	42.44	73.22	103.12	15.26	54
Cottidae indet.						
Atlantic cod	*Gadus morhua* (Linneus, 1758)	67.73	151.08	238.27	34.92	41
Pollack	*Pollachius pollachius* (Linneus, 1758)	103.23	149.74	181.96	19.29	24
Poor cod	*Trisopterus minutus* (Linneus, 1758)	20.33	100.41	216.96	27.11	249
Shore rockling	*Gaidropsarus mediterraneus* (Linneus, 1758)	128.44	164.04	220.73	32.16	7
Saithe	*Pollachius virens* (Linneus, 1758)	21.62	54.39	304.04	27.44	590*
Tadpole fish	*Raniceps raninus* (Linneus, 1758)	85.25	85.25	85.25	-	1
Gadidae indet.		67.39	116.23	167.30	38.49	26
Black goby	*Gobius niger* (Linneus, 1758)	146.61	146.61	146.61	-	1
Gobiidae indet.	(G. Cuvier, 1816)	11.93	29.25	59.84	15.59	13

Corkwing wrasse	*Symphodus melops* (Linneus, 1758)	123.77	142.84	180.96	9.83	8
Cuckoo wrasse	*Labrus mixtus* (Linneus, 1758)	214.14	214.14	214.14	-	1
Golsinny wrasse	*Ctenolabrus rupestris* (Linneus, 1758)	98.09	108.69	123.64	8.86	10
Labridae indet.	(G. Cuvier, 1816)	44.90	80.96	171.26	21.41	264
Common ling	*Molva molva* (Linneus, 1758)					
Rock gunnel	*Pholis gunnel* (Linneus, 1758)	88.21	101.26	123.00	16.66	4
Flatfish	(Linneus, 1758)					
Viviparous eelpout	*Zoarces viviparus* (Linneus, 1758)	101.86	112.62	155.65	24.06	5

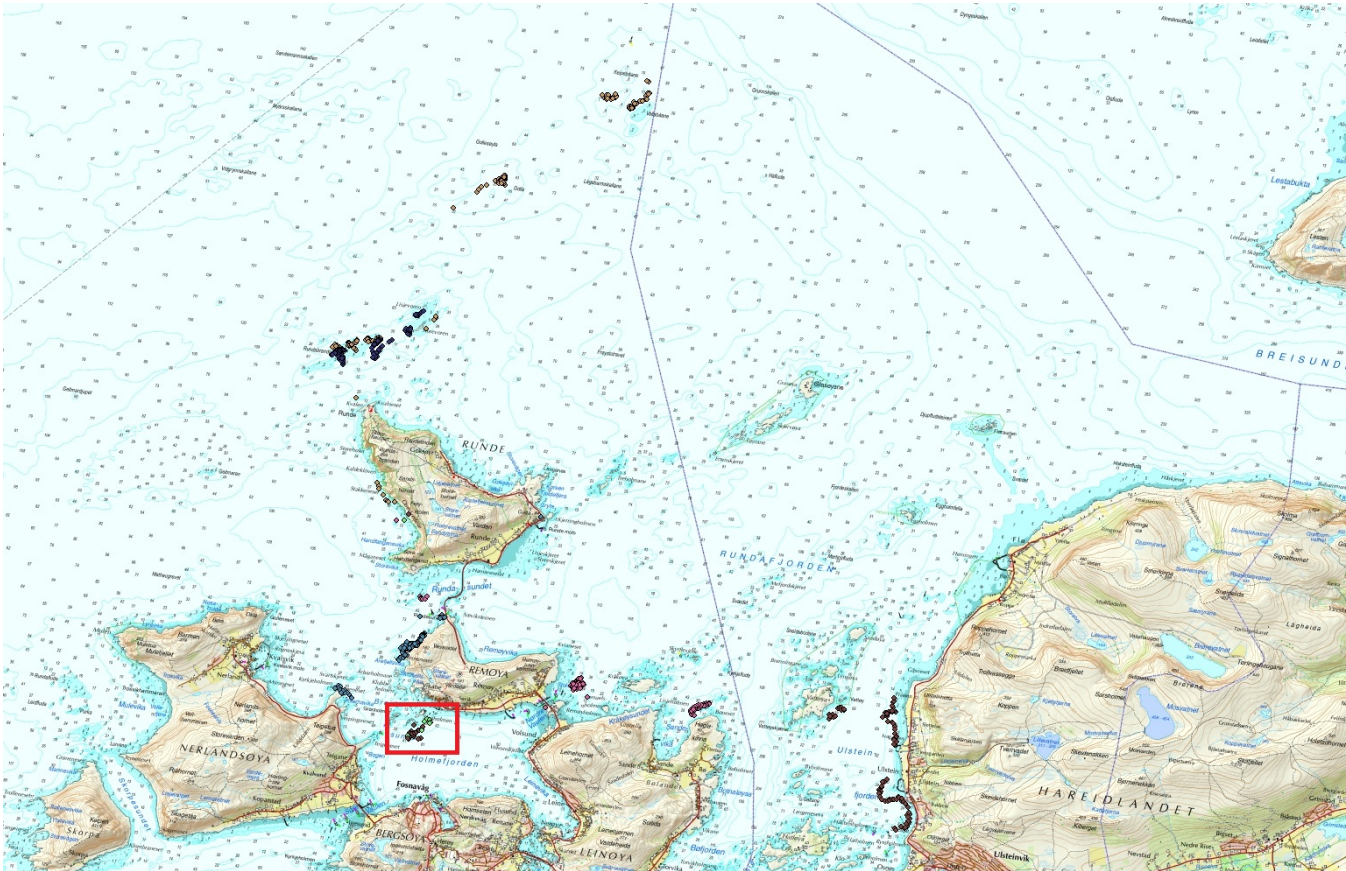# Appendix 5: Map of all shag diving locations

Figure 0.1: GPS locations of shag dives (n=861) from 7 logger units. The red square indicates shag diving activity within the survey area at Remøya. The furthest location is ca. 14km north from the nesting area at Runde, while the most frequented area (23% of dives) is Rundebrandane. No shags dives were recorded the east of Runde, but this is an area of kelp trawling and fish aquaculture, which may impact shag foraging behavior.